

NAVAL POSTGRADUATE SCHOOL

Monterey, California



THESIS

H4237

**THE EFFECT OF AGING TREATMENT
ON THE MICROSTRUCTURE AND PROPERTIES
OF COPPER-PRECIIPITATION
STRENGTHENED HSLA STEEL**

by

Marvin H. Heinze

December 1988

Thesis Co-Advisors:

Saeed Saboury
J. M. B. Losz

Approved for public release; distribution is unlimited.

T241957

Unclassified

Security Classification of this page

REPORT DOCUMENTATION PAGE

1a Report Security Classification Unclassified			1b Restrictive Markings		
2a Security Classification Authority			3 Distribution Availability of Report		
2b Declassification/Downgrading Schedule			Approved for public release; distribution is unlimited.		
4 Performing Organization Report Number(s)			5 Monitoring Organization Report Number(s)		
6a Name of Performing Organization		6b Office Symbol	7a Name of Monitoring Organization		
Naval Postgraduate School		(If Applicable) 33	Naval Postgraduate School		
6c Address (city, state, and ZIP code)			7b Address (city, state, and ZIP code)		
Monterey, CA 93943-5000			Monterey, CA 93943-5000		
8a Name of Funding/Sponsoring Organization		8b Office Symbol	9 Procurement Instrument Identification Number		
		(If Applicable)			
8c Address (city, state, and ZIP code)			10 Source of Funding Numbers		
			Program Element Number	Project No	Task No
			Work Unit Accession No		
11 Title (Include Security Classification) The Effect of Aging Treatment on the Microstructure and Properties of Copper-Precipitation Strengthened HSLA Steel					
12 Personal Author(s) Marvin. H. Heinze					
13a Type of Report		13b Time Covered		14 Date of Report (year, month, day)	
Master's Thesis		From To		December 1988	
15 Page Count					
65					
16 Supplementary Notation The views expressed in this thesis are those of the author and do not reflect the official policy or position of the Department of Defense or the U.S. Government.					
17 Cosati Codes			18 Subject Terms (continue on reverse if necessary and identify by block number)		
Field	Group	Subgroup	HSLA-100		
19 Abstract (continue on reverse if necessary and identify by block number)					
<p>The high strength low alloy (HSLA) steels which are being developed as replacements for the HY family of steels are low carbon steels which derive their strength in part due to the precipitation of fine coherent copper particles formed during a quench and aging heat treatment. HSLA-100 is being developed to meet the strength and toughness requirements of HY-100 but can be easily welded without preheat, thereby reducing fabrication costs. This investigation uses light and electron microscopy for microstructural characterization while tensile, Charpy, and hardness tests are relied upon for the mechanical properties. The microstructure and mechanical characteristics of HSLA-100 after aging at several different temperatures was correlated. A high ductility and the minimum 100 ksi yield strength was found after aging at 675 C, although this temperature was found to be close to the low eutectoid temperature displayed by HSLA-100. Splitting was observed in the tensile fracture surfaces but the mechanical properties were not adversely affected.</p>					
20 Distribution/Availability of Abstract			21 Abstract Security Classification		
<input checked="" type="checkbox"/> unclassified/unlimited <input type="checkbox"/> same as report <input type="checkbox"/> DTIC users			Unclassified		
22a Name of Responsible Individual			22b Telephone (Include Area code)		22c Office Symbol
M. B. Losz			(408) 646-2851		69Lo

DD FORM 1473, 84 MAR

83 APR edition may be used until exhausted

security classification of this page

All other editions are obsolete

Unclassified

Approved for public release; distribution is unlimited.

**The Effect of Aging Treatment on the Microstructure and
Properties of Copper-Precipitation Strengthened HSLA Steel**

by

Marvin H. Heinze
Lieutenant, United States Navy
B.S., University of Virginia, 1980

Submitted in partial fulfillment of the
requirements for the degree of

MASTER OF SCIENCE IN MECHANICAL ENGINEERING

from the

NAVAL POSTGRADUATE SCHOOL
December 1988

ABSTRACT

The high strength low alloy (HSLA) steels which are being developed as replacements for the HY family of steels are low carbon steels which derive their strength in part due to the precipitation of fine coherent copper particles formed during a quench and aging heat treatment. HSLA-100 is being developed to meet the strength and toughness requirements of HY-100 but can be easily welded without preheat, thereby reducing fabrication costs. This investigation uses light and electron microscopy for microstructural characterization while tensile, Charpy, and hardness tests are relied upon for the mechanical properties. The microstructure and mechanical characteristics of HSLA-100 after aging at several different temperatures was correlated. A high ductility and the minimum 100 ksi yield strength was found after aging at 675 C, although this temperature was found to be close to the low eutectoid temperature displayed by HSLA-100. Splitting was observed in the tensile fracture surfaces but the mechanical properties were not adversely affected.

112515
H4237
C.1

TABLE OF CONTENTS

I. INTRODUCTION.....	1
II. BACKGROUND	4
A DEVELOPMENT OF COPPER BEARING HSLA STEELS	4
B ROLES OF ALLOYING ELEMENTS IN HSLA STEELS.....	6
C THE ROLE OF COPPER IN STRENGTHENING HSLA STEELS.....	7
1. Solid Solution Strengthening.....	7
2. Precipitation Strengthening.....	8
D APPLICATIONS OF COPPER-STRENGTHENED HSLA STEELS.....	8
III. EXPERIMENTAL PROCEDURES	10
A MATERIAL	10
B HEAT TREATMENT	10
C MECHANICAL PROPERTIES	11
1. Hardness.....	11
2. Strength and Notch Toughness	11
D MICROSCOPY	13
1. Optical Microscopy.....	13
2. Scanning Electron Microscopy	13
3. Transmission Electron Microscopy.....	13

IV. EXPERIMENTAL RESULTS	15
A. MECHANICAL PROPERTIES	15
1. Hardness.....	15
2. Strength and Notch Toughness	16
B. MICROSTRUCTURE	21
1. As Quenched	21
2. 500 C Aging Temperature.....	23
3. 650 C Aging Temperature.....	29
4. 700 C Aging Temperature.....	33
C. FRACTOGRAPHY	33
1. Tensile Testing.....	33
2. Charpy V-Notch Testing.....	39
V. DISCUSSION.....	48
VI. SUMMARY	53
APPENDIX SPECIFICATION CHEMICAL COMPOSITION AND MECHANICAL PROPERTY REQUIREMENTS FOR NAVAL HULL MATERIALS.....	54
LIST OF REFERENCES.....	55
INITIAL DISTRIBUTION LIST.....	57

ACKNOWLEDGMENTS

I wish to express my appreciation to my thesis advisors, Dr. Saeed Saboury and Dr. J. Mauro Losz, for the patience and guidance they provided in this work. A special thanks goes to Dr. Losz for his transmission electron microscopy and to Dr. Saboury for the late night hours we shared. I would also like to recognize the laboratory support provided by Mr. Tom Kellog and Mr. Rob Hafley while I worked with the Material Science group.

I. INTRODUCTION

The U. S. Navy currently makes extensive use of HY steels in naval ship construction. These steels obtain much of their strength through a quench and aging process, using carbon as the major strengthening element. The welding of these steels is expensive as sustained pre-heat, controlled interpass temperatures, and heat input limitations are necessary to avoid hydrogen-assisted cracking in the coarse heat affected zone of the weld [Ref. 1].

The U. S. Navy has undertaken a program of developing and qualifying a family of low carbon steels for ship construction which will be more easily weldable. These high strength low alloy (HSLA) steels have a low carbon content and use the precipitation of fine copper particles as a strengthening mechanism. The advantage of this alloying design can be seen by consulting the Graville Diagram (Figure 1) [Ref. 2]. The combination of the carbon content and the carbon equivalent yields three zones. Zone III, which is difficult and expensive to weld, includes the HY steels. The copper-precipitation strengthened HSLA steels, because of their lower carbon content, are in Zone I, which is easy to weld without extensive preheat or other expensive preparations. [Ref. 3]

The first of these steels to be approved for ship construction is HSLA-80 (MIL-S-24645). This steel has excellent weldability and

TRADITIONAL NAVY STRUCTURAL STEELS	HY-80 HY-100	C	Mn	P	S	Si	Cr	Ni	Mo	Cu	Cb	V	B	C.E.*
		.15	.25	.01	.01	.25	1.40	2.70	.40	.05	—	.01	—	0.78
		.17	.25	.01	.01	.25	1.40	2.90	.40	.05	—	.01	—	0.81
CURRENT DEVELOPMENT HSLA (CONV. ALLOY)	HSLA-80	.04	.55	.01	.005	.30	0.70	0.90	.20	1.20	.04	—	—	0.50
	HSLA-100	.04	.90	.01	.005	.25	0.60	3.50	.60	1.60	.03	—	—	0.81

*C.E. = CARBON EQUIVALENT

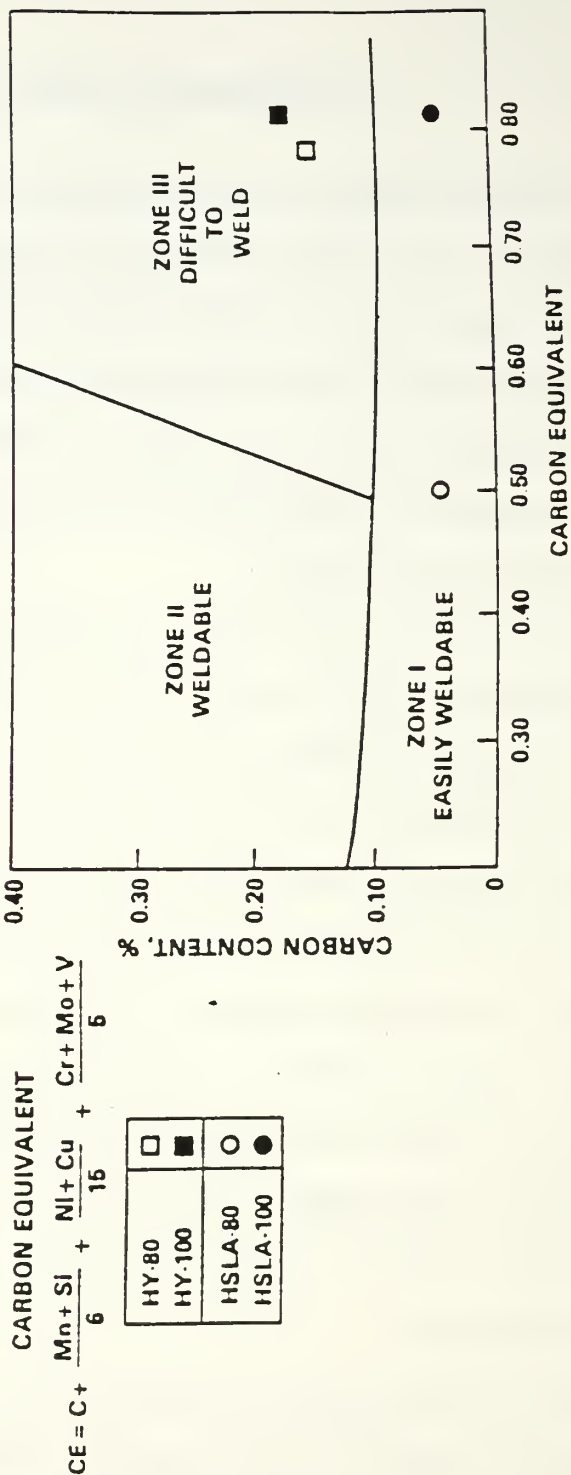


Figure 1. Graville Diagram—Weldability as a Function of Carbon Content and Carbon Equivalent for Some Shipbuilding Materials

toughness and requires no welding preheat at plate thickness up to 19mm (0.75 in) [Ref. 4]. Currently, another steel in this HSLA family is being developed at the 690 MPa (100 ksi) strength level. HSLA-100 is a modification of HSLA-80 in that it contains all of the same alloying elements as HSLA-80 and it is solution treated, quenched, and aged as is HSLA-80. HSLA-100 has greater amounts of nickel, copper, manganese, and molybdenum than HSLA-80, giving HSLA-100 a much higher carbon equivalent. [Ref. 2]

This work examines the effect of aging treatment on the microstructure and mechanical properties of a 25.4 mm (1 inch) thick HSLA-100 steel plate. The microstructure is characterized by light and transmission electron microscopy and mechanical properties evaluated by Charpy V-notch, tensile and hardness testing. Fractography is conducted by scanning electron microscopy.

II. BACKGROUND

A. DEVELOPMENT OF COPPER BEARING HSLA STEELS

Copper has been added to structural steels to provide increased resistance to corrosion and better weathering properties for many years. Although some work on the role of copper in strengthening steels was performed as early as 1929, an understanding of the contribution that copper makes to mechanical properties has been slow in developing. [Ref. 5]

In 1960, Hornbogen examined the precipitation of copper from alpha iron and concluded that the copper precipitates as FCC ϵ -phase without any intermediate compounds being formed. Hornbogen also observed that the copper initially precipitates as spherical particles and that these particles tended to grow in the $[110]_{\epsilon}$ direction. After prolonged aging at higher temperatures, this directional growth forms rod-like particles. In comparing samples quenched from both alpha and gamma regions (Figure 2), Hornbogen found that the only notable difference was that the specimens quenched from the gamma region showed some copper precipitating as a film along subboundaries produced by the transformation from the gamma region. [Ref. 6]

Speich and Oriani explored the rate of coarsening of copper precipitates in an alpha iron matrix. Their research confirmed the

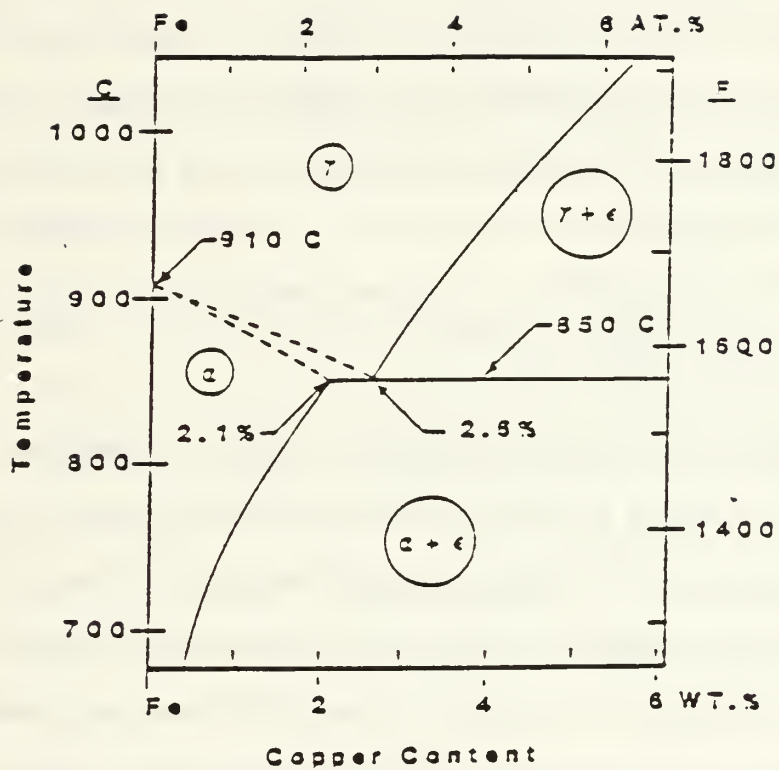


Figure 2. Iron-Rich Portion of Fe-Cu Phase Diagram

rod-like shape found by Hornbogen after prolonged aging and concluded that the equilibrium shape of the copper particles is one of rods with hemispherical caps. [Ref. 7]

In 1973, Goodman and co-workers observed that a Fe-Cu alloy reaches its peak strength upon aging well before precipitation is complete. Goodman also found that the number of the particles decreases rapidly after the peak strength of the alloy is reached. Through field-ion microscopy, the mean diameter of the particles at the maximum strength were found to be about 24 angstroms. Goodman also determined that at the peak hardness, the precipitate particles were only 40 to 60 percent copper, but that in the overaged condition the particles approached the equilibrium composition of the ϵ -phase, which is nearly pure copper. [Refs. 8, 9]

B. ROLES OF ALLOYING ELEMENTS IN HSLA STEELS

Copper and nickel are the principal alloying elements in HSLA-100 steel. Copper is the primary strengthening precipitate and nickel modifies the ferrite matrix to reduce the tendency of copper to create hot shortness problems in steel. Without nickel in sufficient quantities, the copper will segregate at rolling temperatures and cause the steel to break up as the copper wets the austenite grain boundaries [Ref.10]. Nickel also helps improve the toughness properties of HSLA-100 steel. [Refs. 4,11]

Chromium, manganese, and molybdenum are used to control the grain size and strengthen the ferrite matrix by suppressing polygonal ferrite formation and allowing acicular bainitic ferrite to form instead

[Ref. 4]. Chromium and molybdenum favorably influence the precipitation kinetics of the copper by retarding the copper precipitation during cooling from the austenite range. Chromium also contributes to the corrosion resistance of the alloy [Ref. 12].

Niobium acts as a grain refinement agent to control the austenite grain growth during hot rolling and austenitizing [Ref. 4]. Aluminum also acts as a grain refinement agent and silicon is added as a deoxidizer [Ref. 13].

Carbon is kept low to improve the weldability of HSLA-100. Sulfur content is kept as low as possible to prevent its adverse effect on toughness [Ref. 4].

C. THE ROLE OF COPPER IN STRENGTHENING HSLA STEELS

From Figure 2, it can be seen that upon cooling alloys of iron and copper, the products of the eutectoid reaction are epsilon phase FCC copper and alpha phase iron. The maximum solubility of copper in iron is 2.1 percent at approximately 850 C. Precipitation strengthening is possible because the solubility of copper in iron decreases as temperature decreases. Although very little information has been reported about the effect of copper on the transformation kinetics and hardenability of steels, it has been reported that copper lowers the M_s temperature slightly and delays the decomposition of austenite. [Ref. 14]

1. Solid Solution Strengthening

Dissolved copper atoms cause some solid solution strengthening of ferrite, although the total effect is small. Copper may raise the

yield point of ferrite up to 3.8 MPa for each 0.1% Cu which is present in solution. [Ref. 14]

2. Precipitation Strengthening

As the solubility of copper decreases with decreasing temperature, ϵ -phase can be precipitated by aging the supersaturated alpha phase formed during rapid cooling (water quench). This process involves the formation and growth of coherent BCC copper clusters, their transformation to FCC epsilon phase spherical particles, and the growth of these particles into rod-like shapes on prolonged aging [Ref. 14]. Various sites have been reported for the epsilon phase precipitation, with uniform precipitation being found most often [Ref. 6]. Precipitation strengthening can cause a significant increase in the strength of ferrite, with increments of 248 MPa per 1 percent Cu being obtainable [Ref. 14]. Hornbogen suggested that this strengthening may be created by copper clusters causing jogs in screw dislocations reducing dislocation mobility [Ref. 14]. Numerous explanations have been offered for this strengthening, but the mechanisms causing the strengthening are still uncertain.

D. APPLICATIONS OF COPPER-STRENGTHENED HSLA STEELS

Copper-strengthened HSLA steels are seeing more widespread use as the roles of copper are more clearly understood. Copper-containing HSLA steels have been used in pipelines, storage tanks, fittings, and naval structures. HSLA-80 has been used in off-shore oil platforms in addition to U.S. Navy ships of the Ticonderoga (CG-47) class [Ref. 5]. The use of HSLA-80 in the Ticonderoga class has

resulted in savings of 5 to 15 percent in the as fabricated steel cost due to reduced plate and preheating costs [Ref. 2]. The cost savings and increasing strengths being obtained in copper precipitation-strengthened HSLA steels will see them utilized in a wide range of future applications.

III. EXPERIMENTAL PROCEDURES

A. MATERIAL

A 25.4 X 406.4 X 609.6 mm plate of HSLA-100 steel was provided by David W. Taylor Naval Ship Research and Development Center, Annapolis, Maryland (DTRC). This plate (DTRC code GLC) was manufactured by Phoenix Steel Corporation, Claymont, Delaware. Table 1 identifies the plate chemistry as determined by the manufacturer [Ref. 15]. From this plate, 17 blanks were cut which were 27.0 x 25.4 x 203.2 mm. The blanks were taken from the plate such that the 203 mm length was parallel to the plate rolling direction.

TABLE 1

GLC PLATE COMPOSITION

C	Mn	P	S	Si	Cu	Ni	Cr	Mo	Al	Nb
.04	.86	.004	.002	.27	1.58	3.55	.57	.60	.032	.029

B. HEAT TREATMENT

Fifteen of the 17 blanks were austenitized at 915 C for one hour and water quenched. One of the austenitized blanks was utilized for initial hardness tests. The remaining 14 were divided into seven groups of two blanks each. Six of the groups were then aged for one hour at the following temperatures: 500, 600, 625, 650, 675, and 700 C, then water quenched. In the development studies of HSLA-100, it was found that water quenching is necessary in order to meet the U.S. Navy strength and toughness requirements [Ref. 4]. The remaining two

groups were kept in the as-received and as-quenched conditions. All heating was done in a Blue M model 8655F-3 box type furnace under normal atmosphere, with temperatures maintained within ± 3 C.

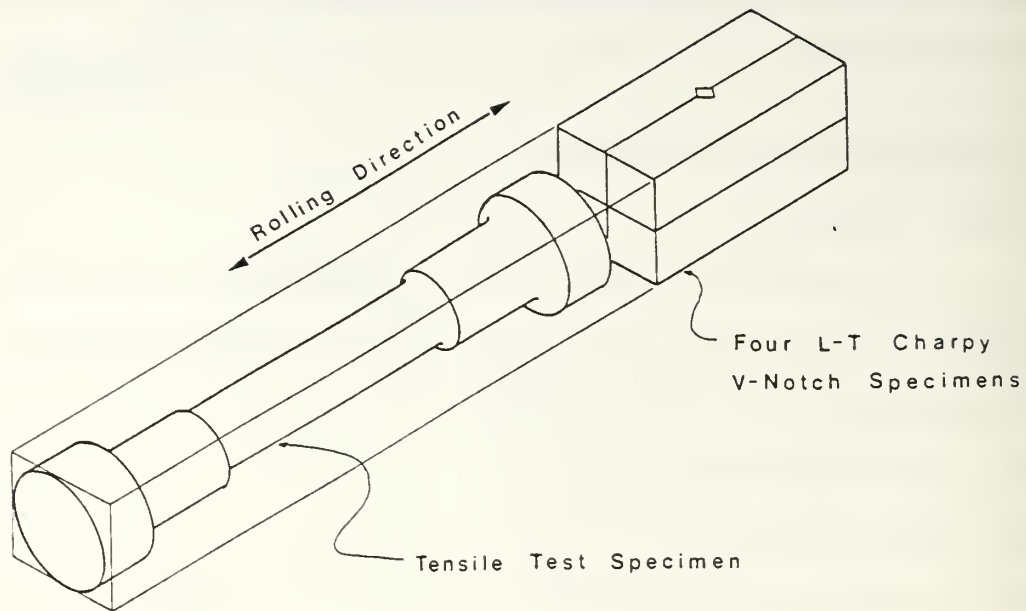
C. MECHANICAL PROPERTIES

1. Hardness

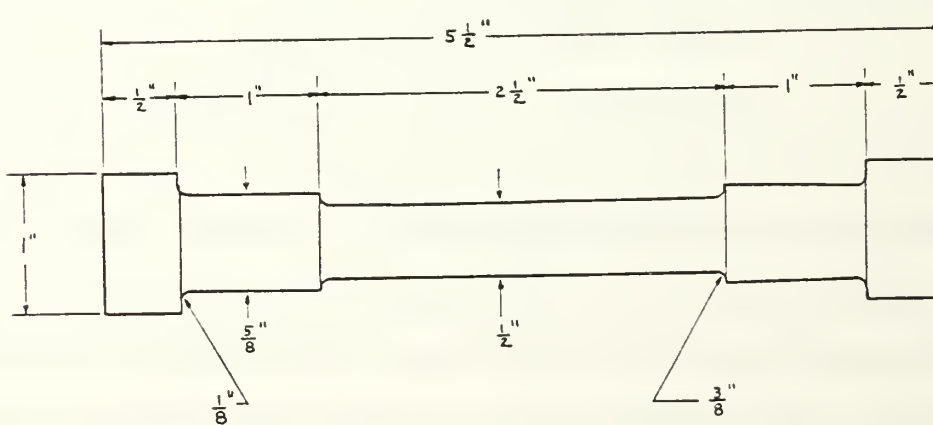
One of the quenched blanks was subdivided into smaller samples (25 x 25 x 10 mm) and aged at the following temperatures: 200, 290, 400, 450, 475, 500, 525, 550, 600, 650, and 700 C. Hardness tests were conducted using a Wilson Rockwell hardness tester on a Rockwell C scale. From the data obtained in the hardness testing, aging temperatures were selected for the heat treatment of the 12 other blanks.

2. Strength and Notch Toughness

After heat treatment, the blanks were machined into round 12.7 mm diameter x 60 mm gage length tensile test specimens and 10 x 10 x 50 mm Charpy V-notch specimens (Figure 3). The blanks were cut in the rolling direction, as explained before, so that the tensile specimens were tested in that direction. The Charpy specimens were cut from the blanks such that they were fractured in the L-T orientation. Tensile testing was carried out at room temperature (20 C) at a strain rate of 7.41×10^{-4} per second on an Instron Model 6027 test apparatus with a Hewlett-Packard 3852A data acquisition control unit and a Hewlett-Packard 7475A plotter to determine strength and



a



b

Figure 3. (a) Schematic of Tensile and Charpy Specimens Cut from the Blanks; (b) Tensile Test Specimen

ductility. Two tensile tests were carried out for each aging temperature. The Charpy specimens were impact tested at three temperatures, 20 C (68 F), -18 C (0 F), and -85 C (-120 F). At least two impact tests were performed at each temperature.

D. MICROSCOPY

1. Optical Microscopy

Metallographic samples from each tensile test specimen (sliced perpendicular to the rolling direction) were mounted, polished, and etched for approximately 29 seconds using a two percent nital solution. Each sample was examined in a Zeiss ICM405 photomicroscope.

2. Scanning Electron Microscopy

Fracture surfaces of each of the Charpy and tensile test specimens were examined in a Cambridge Stereo Scan S4-10 Scanning Electron Microscope operated at 20 KV. Polished and etched surfaces of each extreme of the aging temperatures (500 and 700 C) were also examined for grain structure information.

3. Transmission Electron Microscopy

Samples of each aging temperature, as received, and as quenched conditions were prepared for examination on a transmission electron microscope. Slices, 0.25 millimeter thick, were cut out of each fractured tensile specimen perpendicular to the rolling direction of the plate using a low-speed diamond wafering saw. Each slice was then thinned to approximately 0.15 millimeters by gentle abrasion on wet 600 grade silicon carbide paper. Discs, of three millimeter

diameter, were punched and subsequently thinned to approximately 0.06 millimeters on 600 grade silicon carbide paper in order to remove any corrosion and provide a uniform thickness. These discs were thinned to perforation in a Struers Tenupol electropolishing device with a 10 percent perchloric acid, 90 percent glacial acetic acid solution as electrolyte at an applied voltage of 50 volts and a current of 180 mA at 13 C. The foils were examined on a JEOL model JEM 120CX transmission electron microscope operated at 120KV.

IV. EXPERIMENTAL RESULTS

A. MECHANICAL PROPERTIES

1. Hardness

The variation of the Rockwell C hardness as a function of aging temperature is presented in Figure 4. The maximum hardness occurs near 500 C and the hardness decreases as the aging temperature is increased to 700 C. Goodman and coworkers observed [Ref. 8] that the peak strength is reached well before precipitation is complete. This encouraged the examination of overaged conditions of this steel. The subsequent aging was performed at temperatures from 500 C to 700 C in order to investigate HSLA-100 at its peak strength and in various overaged conditions.

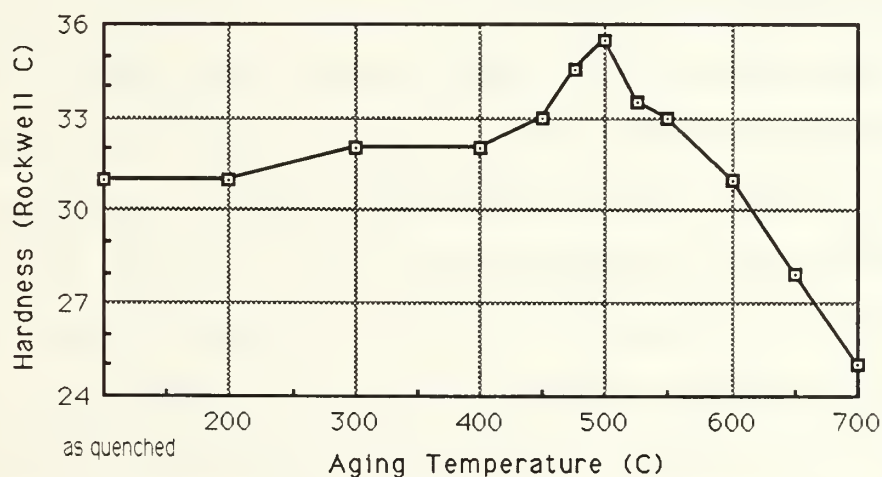


Figure 4. The Effect of Aging Temperature on Hardness

2. Strength and Notch Toughness

Results of the tensile testing are summarized in Table 2. This table includes yield strength, ultimate tensile strength, elongation, and reduction in area measurements. Variations in yield strength and ultimate strength are graphically presented in Figures 5 and 6. Both yield strength and ultimate strength reach a maximum at 500 C aging temperature and then decrease at higher aging temperatures. The strength of all the samples quenched and aged at 500 C to 675 C exceeds the minimum 100 ksi strength requirement that the Navy has set for HSLA-100 steel (Appendix A). Of note is the fact that above 675 C, the ultimate tensile strength rises while the yield strength continues to decrease.

The effects of aging temperature on ductility can be seen in Figure 7. As this figure shows, the ductility of HSLA-100 increases as the aging temperature is increased, reaching a maximum value near an aging temperature of 675 C. Above the 675 C aging temperature, the ductility begins to decline. The variation of ductility and strength from the 675 C to 700 C aging temperatures implies a significant microstructural change in this temperature range. The results of the Charpy impact tests are summarized in Table 3. For better clarity, Figure 8 displays the variation of impact energy with aging temperature for each of the three fracture temperatures. As the testing temperature is lowered, the impact energy decreases. At all aging temperatures, with the exception of the 500 C temperature, HSLA-100 exhibits a

TABLE 2

TENSILE TEST RESULTS

	YIELD STRENGTH MPa (ksi)	ULTIMATE TENSILE STRENGTH MPa (ksi)	ELONGATION (% in 60mm)	REDUCTION OF AREA %	YS/UTS
AS RECEIVED	766 (111.1)	803 (116.4)	21.5	74	.95
AS QUENCHED	787 (114.1)	976 (141.5)	15	72	.81
500C Q&T (932F)	965 (139.9)	1031 (149.5)	18	66.5	.94
600C Q&T (1112F)	887 (128.9)	908 (131.7)	19.5	73	.98
625C Q&T (1157F)	862 (125.0)	875 (126.9)	20	75.5	.99
650C Q&T (1202F)	818 (118.6)	824 (119.5)	20	76.5	.99
675C Q&T (1247C)	752 (109.0)	790 (114.6)	20.5	77	.95
700C Q&T (1292F)	617 (89.5)	804 (116.6)	20	75	.76

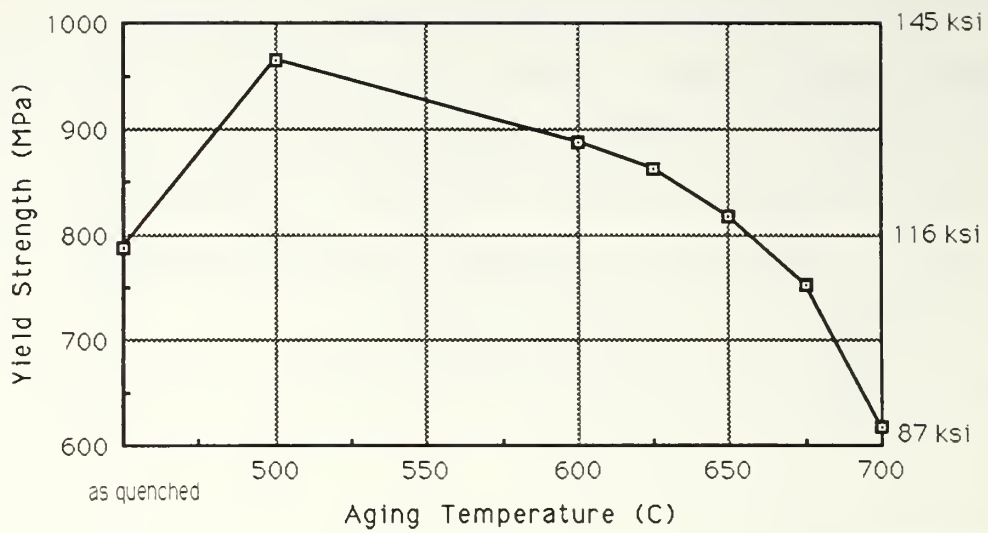


Figure 5. The Effect of Aging Temperature on Yield Strength

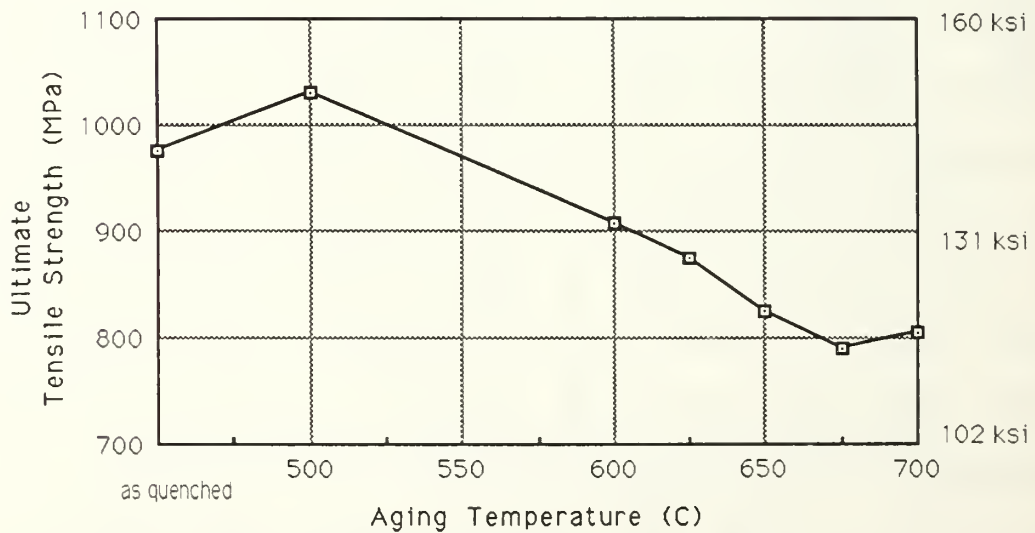


Figure 6. The Effect of Aging on Ultimate Tensile Strength

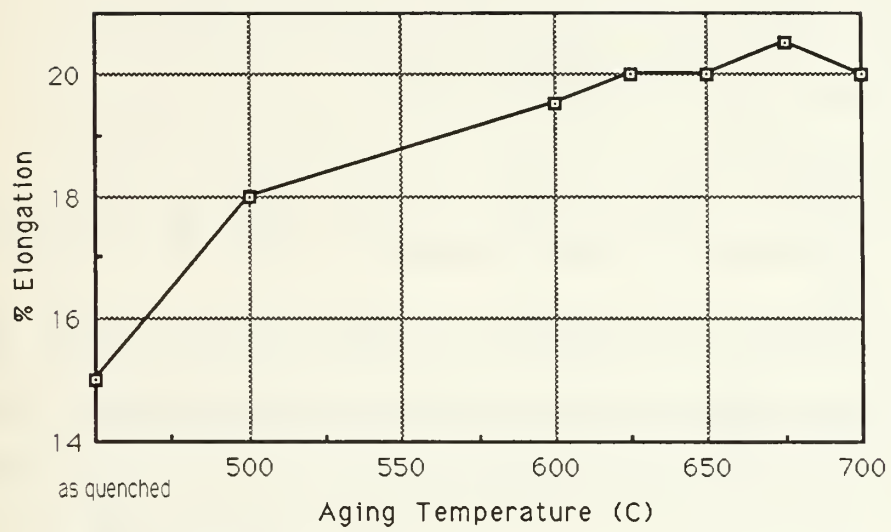


Figure 7. The Effect of Aging Temperature on Ductility

TABLE 3

CHARPY V-NOTCH RESULTS

	20 C (68 F) J (ft-lbs)	-18 C (0 F) J (ft-lbs)	-85 C (-102 F) J (ft-lbs)
AS RECEIVED	97 (179)	125 (170)	97 (131)
AS QUENCHED	108 (146)	102 (137)	92 (125)
500C Q&T (932F)	63 (85)	42 (31)	11 (15)
600C Q&T (1112F)	119 (162)	116 (157)	102 (138)
625C Q&T (1157F)	122 (165)	125 (170)	103 (140)
650C Q&T (1202F)	137 (186)	134 (182)	124 (169)
675C Q&T (1247F)	143 (194)	141 (191)	125 (169)
700C Q&T (1292F)	122 (166)	116 (157)	114 (155)

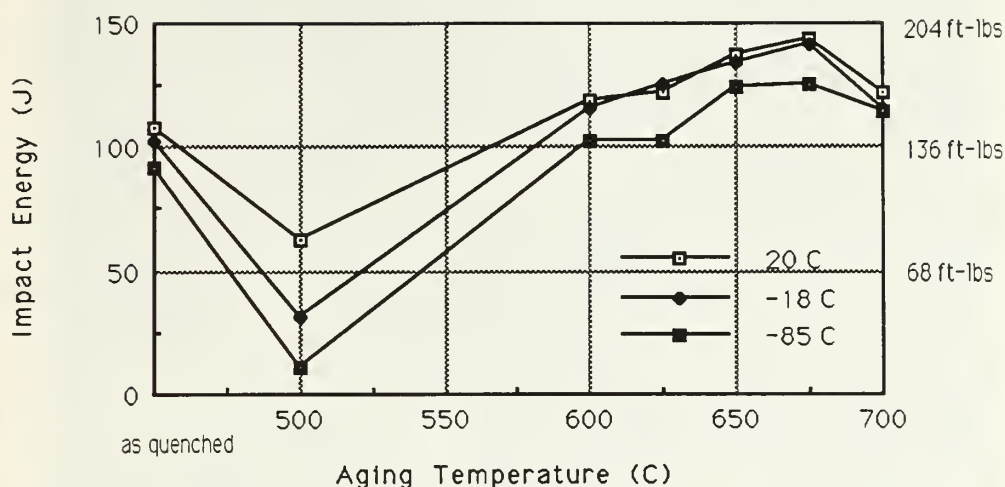


Figure 8. The Effect of Aging Temperature on Notch Toughness

high-impact energy. Impact energies for all of the samples except the 500 C aging temperature exceed the Navy requirements of 26 J (35 ft-lbs) at -85 C (-120 F) and 44 J (60 ft-lbs) at -18 C (0 F).

B. MICROSTRUCTURE

1. As Quenched

A light micrograph of the HSLA-100 in the as-quenched condition is shown in Figure 9. The high-angle boundaries visible are prior austenite grain boundaries which are shown in various degrees of delineation by the two percent nital etch. The scanning electron micrograph in Figure 10 shows the grain structure and precipitate particles in greater detail. Within each prior austenite grain, an



Figure 9. **Light Micrograph of As-Quenched Material, Nital Etch**

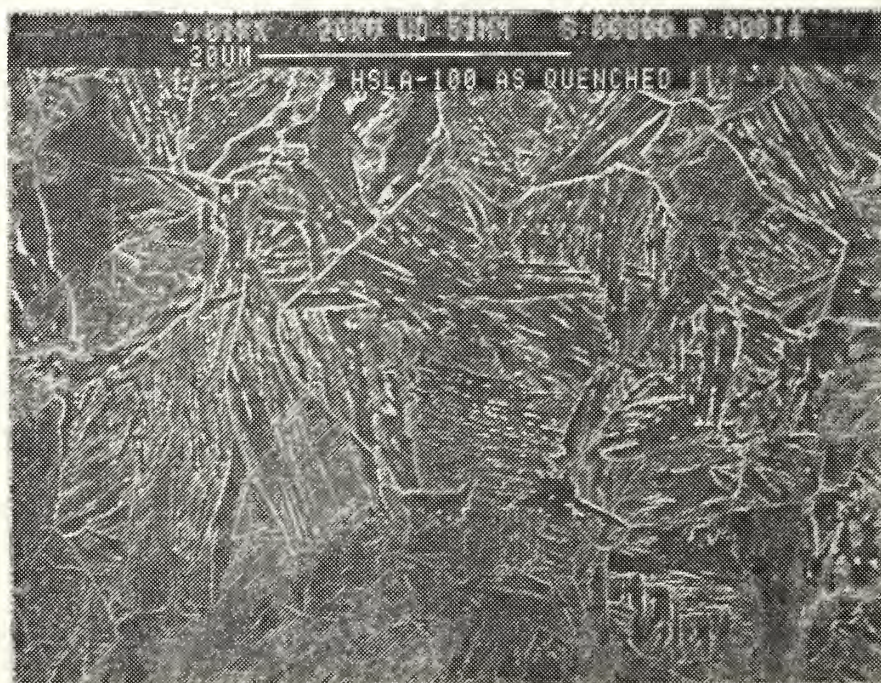


Figure 10. **SEM Micrograph of As-Quenched Material, Nital Etch**

arrangement of parallel laths is visible. From this figure, the spacing of the precipitate particles can be estimated at approximately one micron. Similar microstructures are often referred to as upper bainite [Ref. 16]. In upper bainite, however, cementite particles are found between the ferrite laths. Since HSLA-100 has a low carbon content, it is unlikely that enough cementite can precipitate to cause all of these particles seen in Figure 9. Various researchers [Refs. 16, 17] have identified this structure as granular bainite. Granular bainite consists of a ferrite matrix with a distribution of second-phase particles which are retained austenite or a combination of retained austenite and martensite [Ref. 18]. Figure 11 is a thin foil transmission electron micrograph which shows a prior austenite grain with the ferrite lath structure. The parallel ferrite lath structure is also clearly visible in Figure 12. The area around A shows a high dislocation density. The as-quenched samples have some retained austenite, as shown in the bright field and dark field micrographs in Figure 13. The dark field micrograph was taken using the $(002)_\gamma$ diffraction spot. Twins were observed in ferrite laths, as represented by Figure 14.

2. 500 C Aging Temperature

A light micrograph of the 500 C aged material is shown in Figure 15. The individual laths are not readily resolved by the etching technique in this micrograph, but the particles appear similar to the as-quenched material. Figure 16 shows a transmission electron micrograph of the lath structure. The high dislocation density is apparent by



Figure 11. TEM Micrograph of As-Quenched Material, Prior Austenite Grain Boundaries Visible

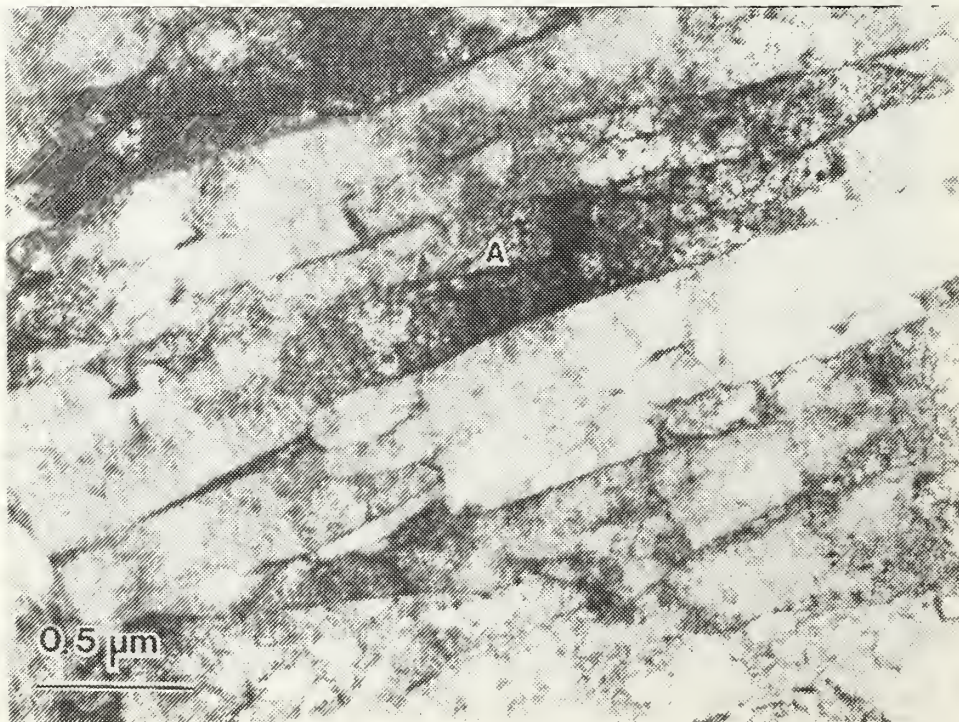


Figure 12. TEM Micrograph of As-Quenched Material

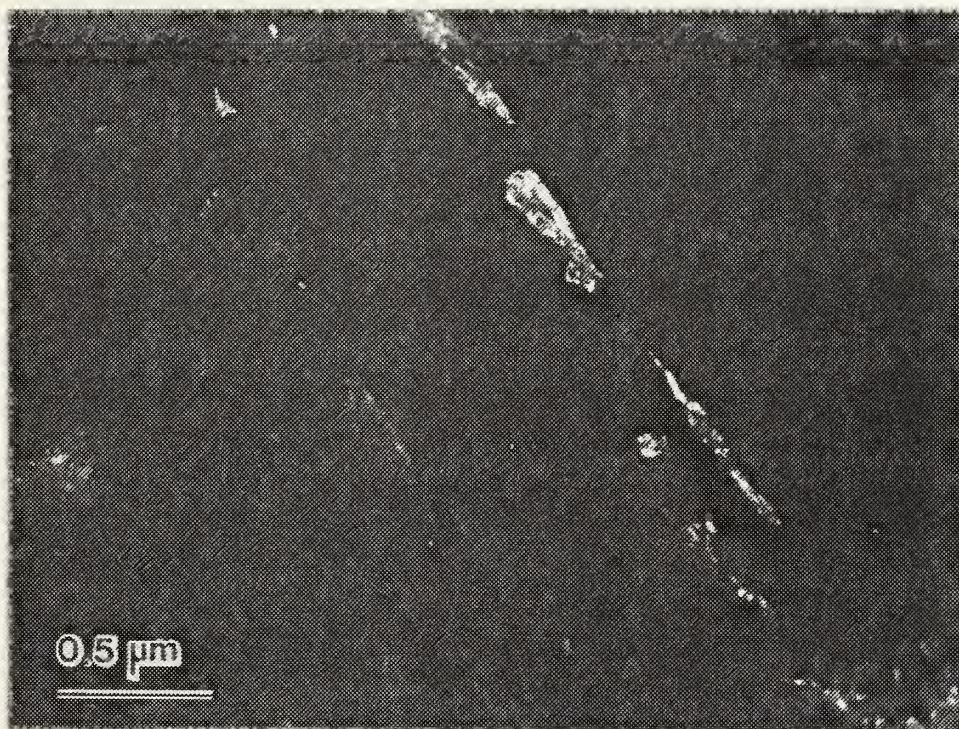
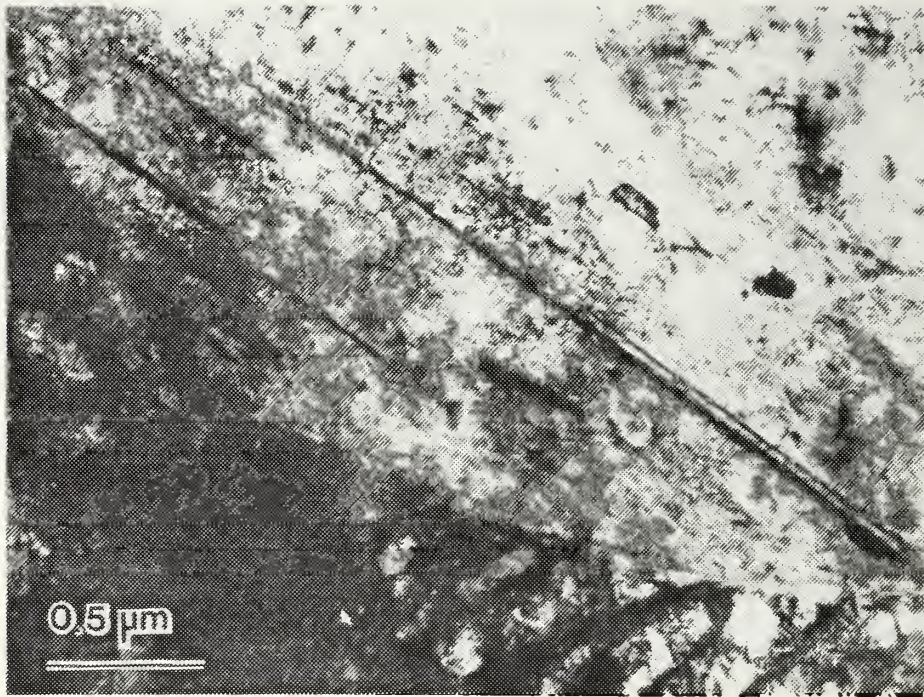


Figure 13. TEM Bright Field/Dark Field Micrographs Showing Retained Austenite



**Figure 14. TEM Bright Field/Dark Field Micrographs
Showing Retained Austenite**

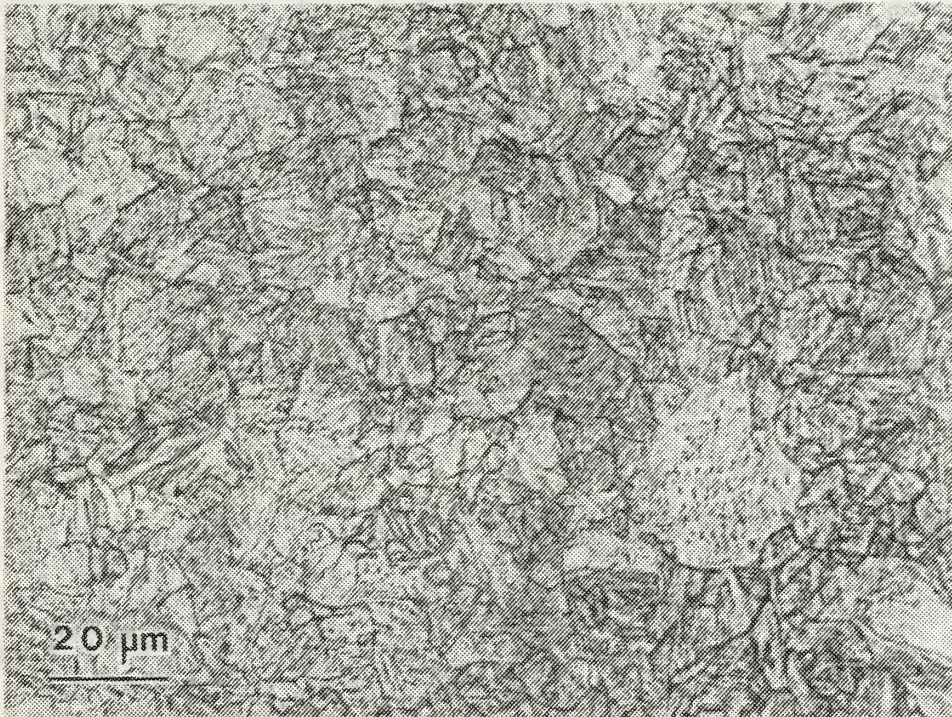
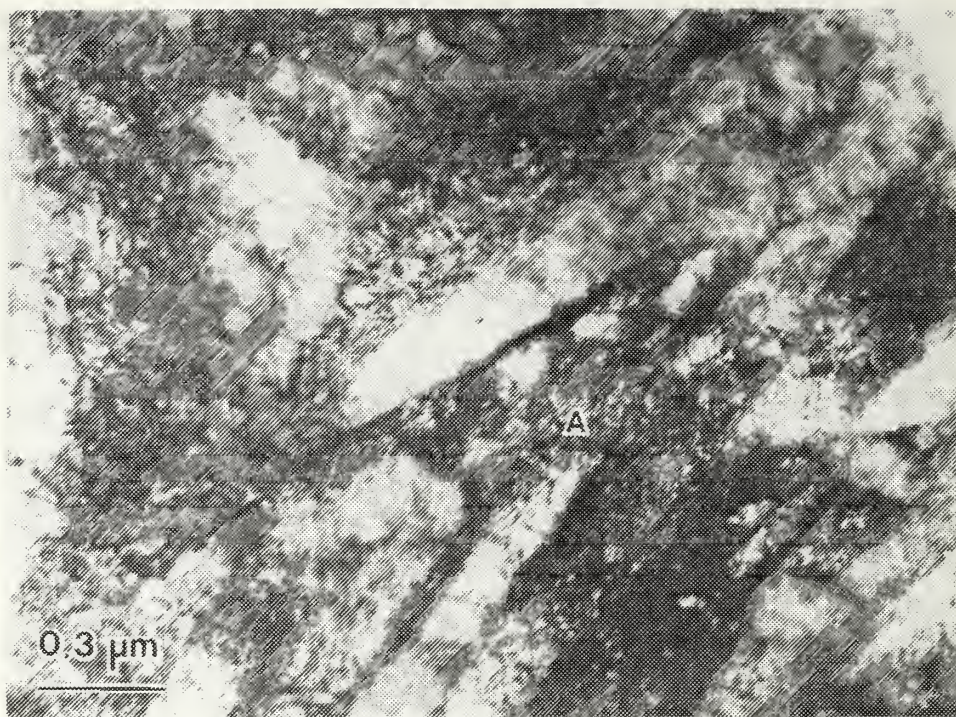


Figure 15. Light Micrograph of 500 C Aged Material, Nital Etch



**Figure 16. TEM Bright Field/Dark Field Micrographs
High Dislocation Density and Retained Austenite**

the dark areas near A. The ferrite lath structure with some microconstituents along the lath boundaries is visible. In the dark field micrograph of Figure 16, retained austenite can be easily discerned. Diffraction patterns indicate that the particle in Figure 17 contains microtwins indicating a high carbon area. The particle in the dark field shown in Figure 18 is high carbon martensite, which was found at isolated locations in the ferrite laths. The 500 C aged material has fine copper precipitates which lack a intense strain field and are not readily resolvable at this magnification [Ref. 19].

3. 650 C Aging Temperature

The light micrograph of 650 C aged material does not reveal any significant differences when compared with the previous conditions (Figure 19). A closer examination of the lath structure in Figure 20 again shows a high density of dislocations. In the area between the laths (A), microconstituents are visible which are probably martensite/austenite. Figure 21 illustrates a large ferrite area with the surrounding lath structure. A uniform distribution of copper particles is visible throughout the ferrite matrix in this figure. These copper particles have diameters from 100 to 300 Å, although many small copper particles are not observable. Coarse copper precipitates are found in localized regions and are prominent in Figure 22. Measurement of these precipitates shows diameters ranging from 200 to 600 Å.

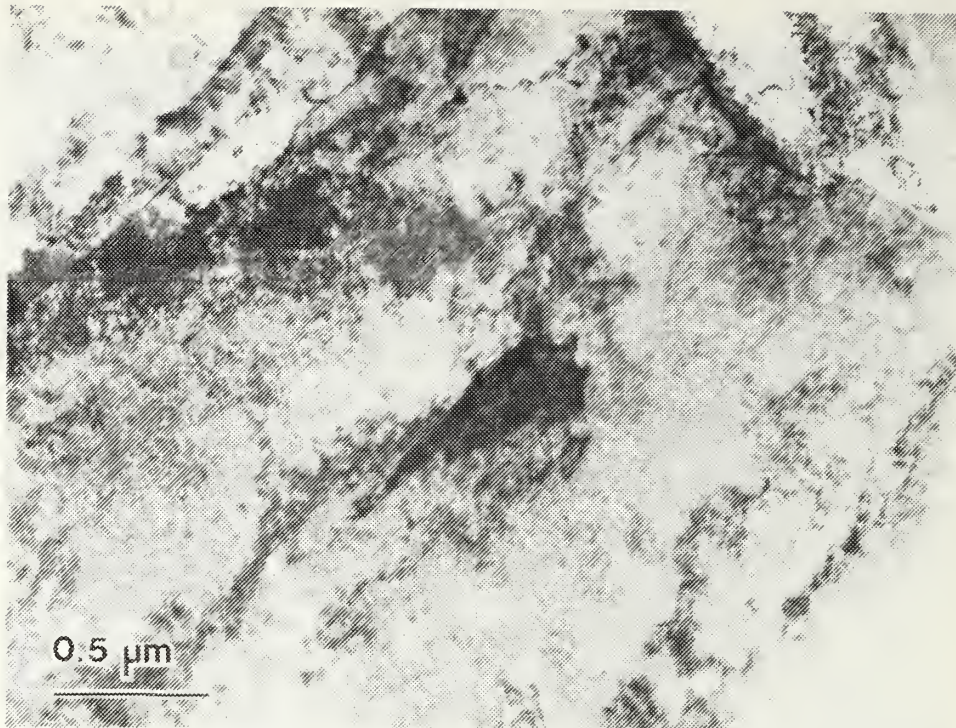


Figure 17. TEM Micrograph of High-Carbon Particle, 500 C Aged Material

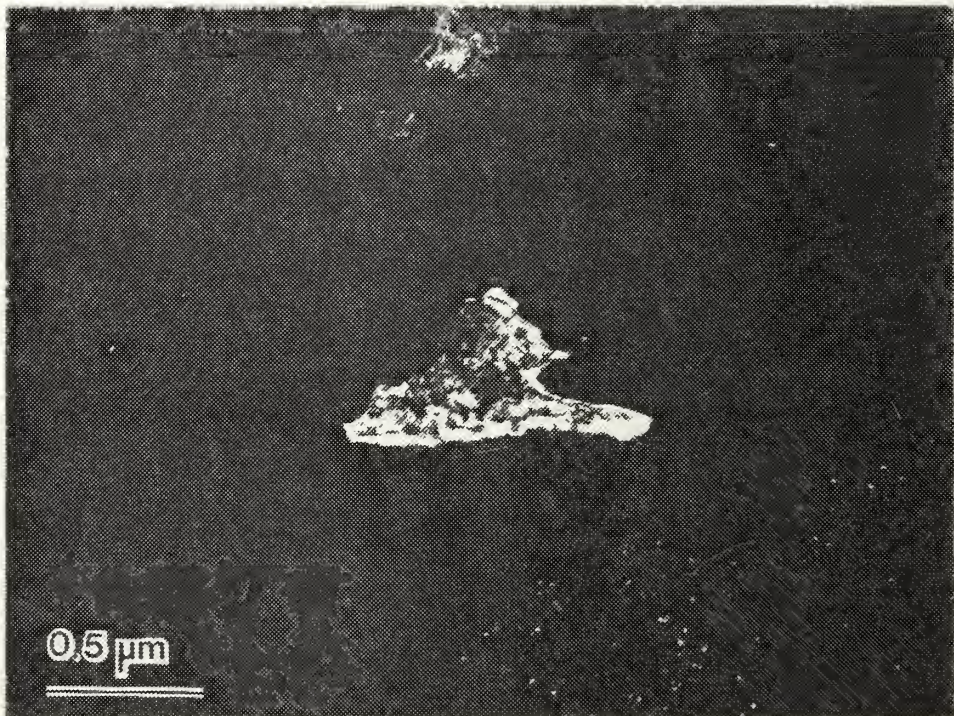


Figure 18. SEM Dark Field Micrograph of Martensite Particle in 500 C Aged Material

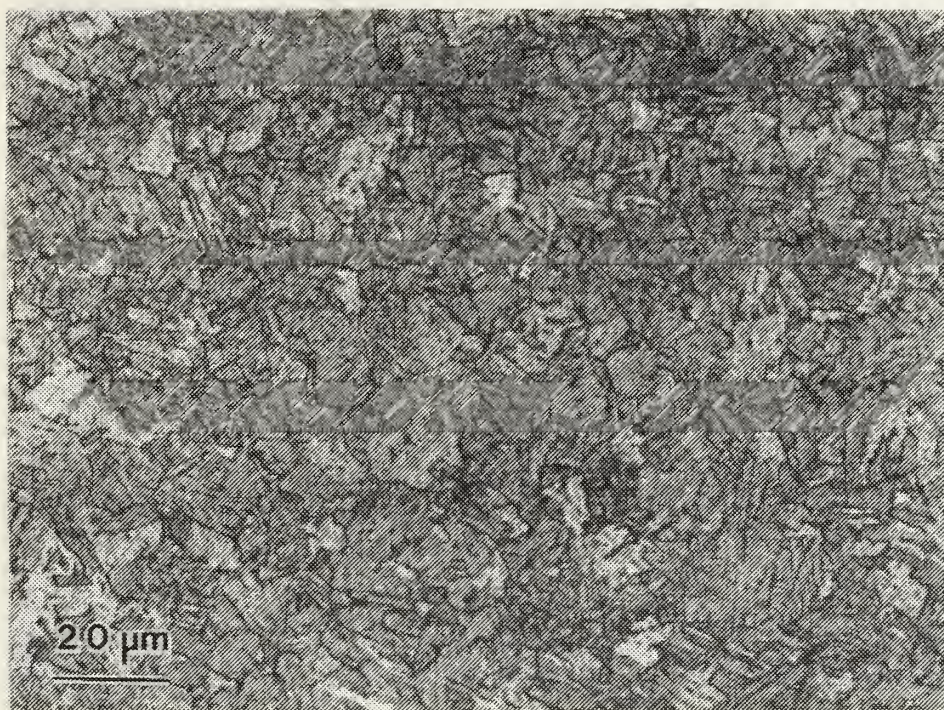


Figure 19. Light Micrograph of 650 C Aged Material, Picral Etch

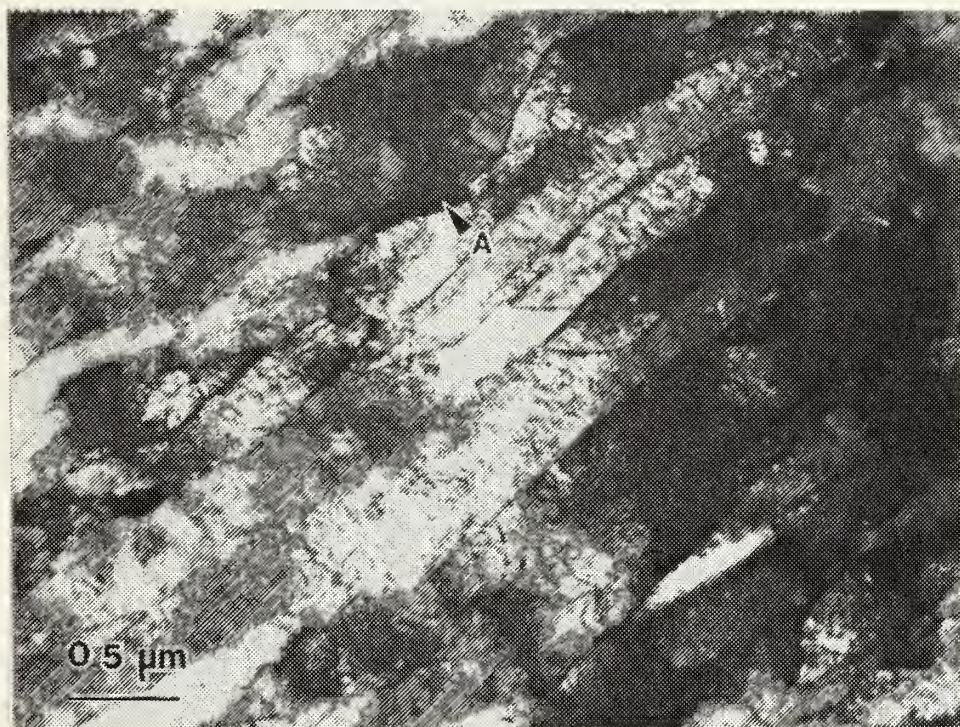


Figure 20. SEM Micrograph of the 650 C Aged Material

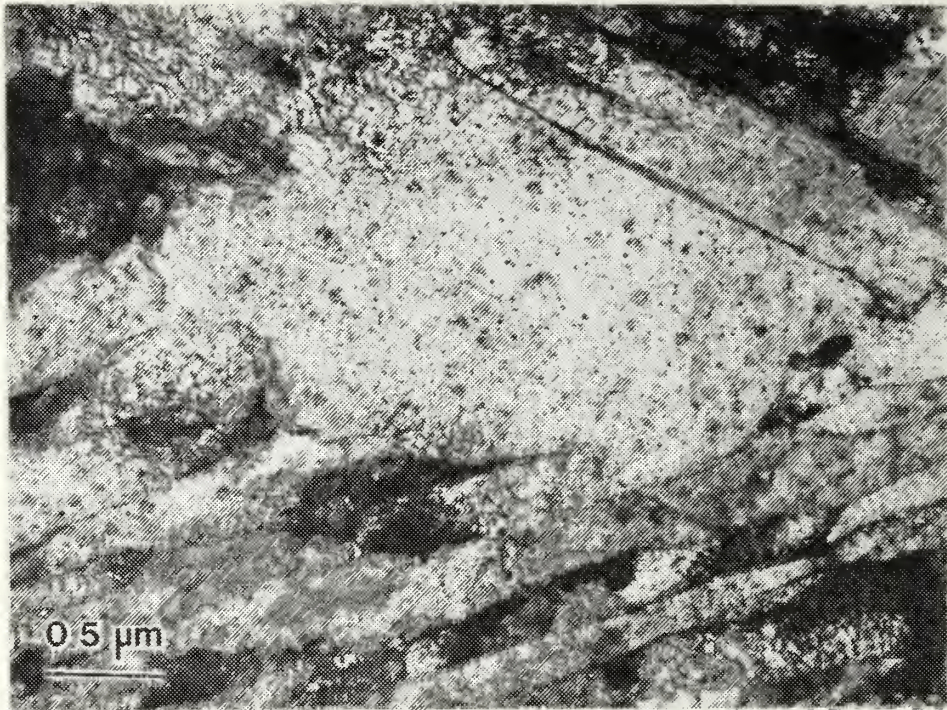


Figure 21. **TEM Micrograph of Ferrite Grain and Lath Structure in 650 C Aged Material**

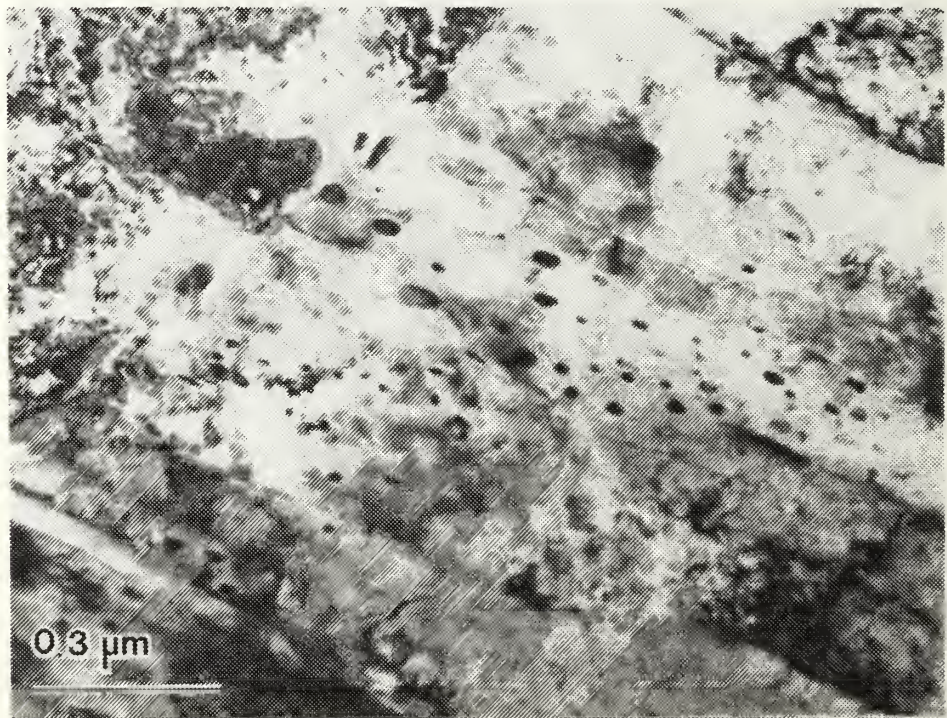


Figure 22. **TEM Micrograph of 650 C Aged Material Showing Copper Precipitates**

4. 700 C Aging Temperature

Figure 23, a light micrograph of the material aged at 700 C, shows that more precipitate particles are visible than were seen at the lower aging temperatures. The dark area at the bottom of Figure 23 indicates some banding effect, possibly caused by manganese segregation [Ref. 2]. An examination of the lath structure in Figure 24 shows a low dislocation density, copper precipitates, and the presence of large amounts of a microconstituent. The microconstituent, which is also visible in Figure 25, was identified as martensite/austenite, which is distributed along the ferrite laths and the grain boundaries. The diffraction patterns for the martensite/austenite particles indicate that the majority of them contain microtwins. These microtwins are visible at T in Figure 26. Figure 27 is a bright field and dark field micrograph which shows a group of coarse copper particles that are as large as 1,000 Å in diameter.

C. FRACTOGRAPHY

1. Tensile Testing

Tensile tests showed that all samples failed in a ductile manner. Figure 28, which shows the tensile fracture surface of HSLA-100 in the as-quenched condition, indicates failure by microvoid coalescence. The classic cup and cone fracture is indicative of a highly ductile condition for this material. The 500 C aged material (Figure 29) exhibits multiple splits in the rolling direction. Although the reasons for this behavior are not precisely understood, various possible causes

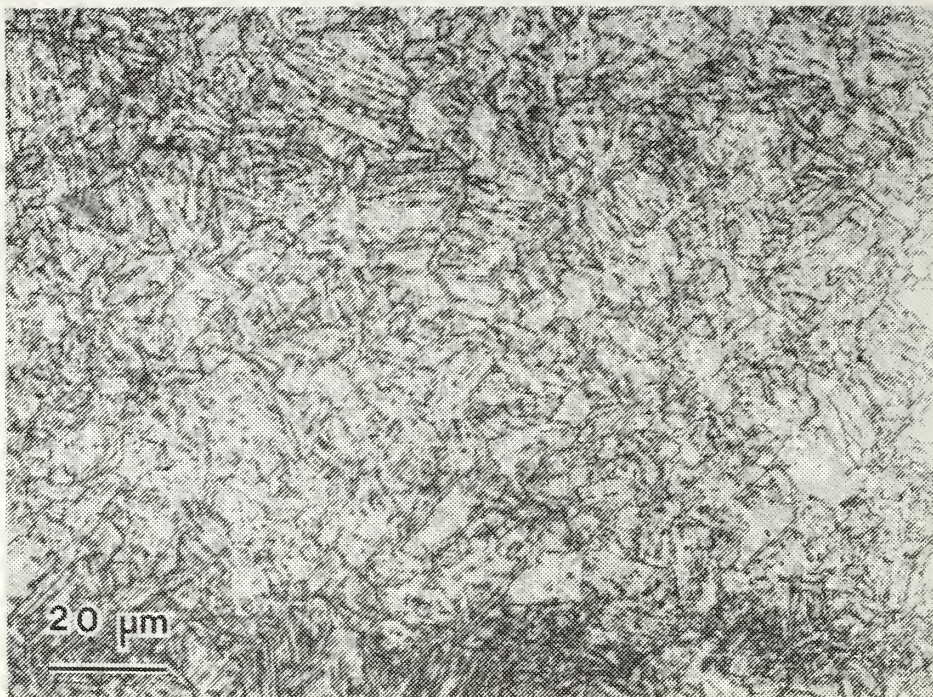


Figure 23. Light Micrograph of 700 C Aged Material, Nital Etch

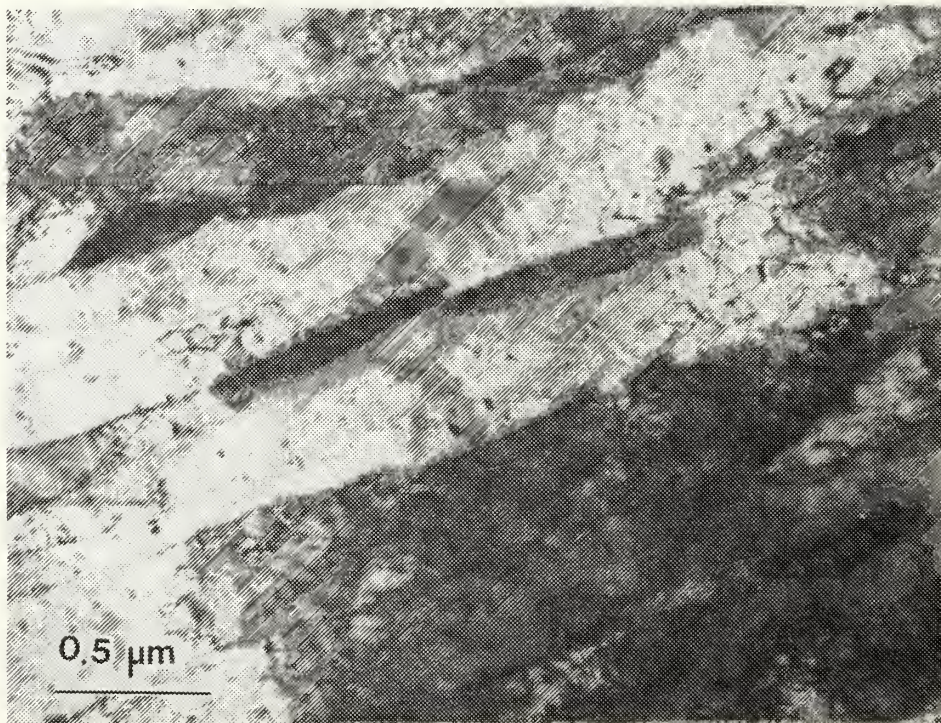


Figure 24. TEM Micrograph of Martensite/Austenite Particles, 700 C Aged Material

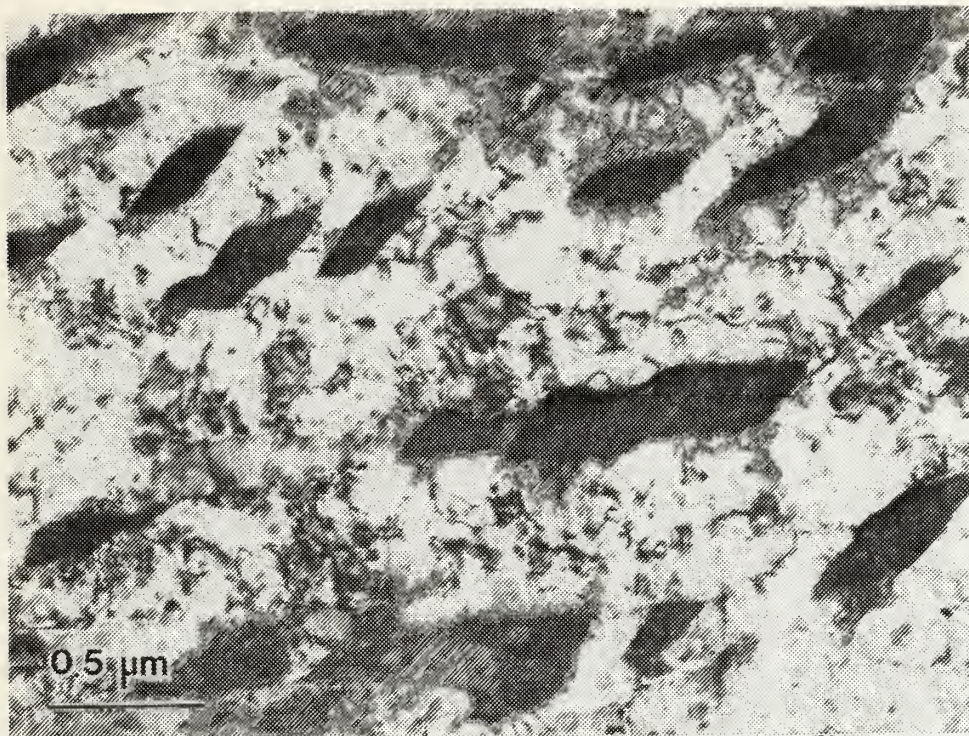


Figure 25. TEM Micrograph of Martensite/Austenite Particles, 700 C Aged Material

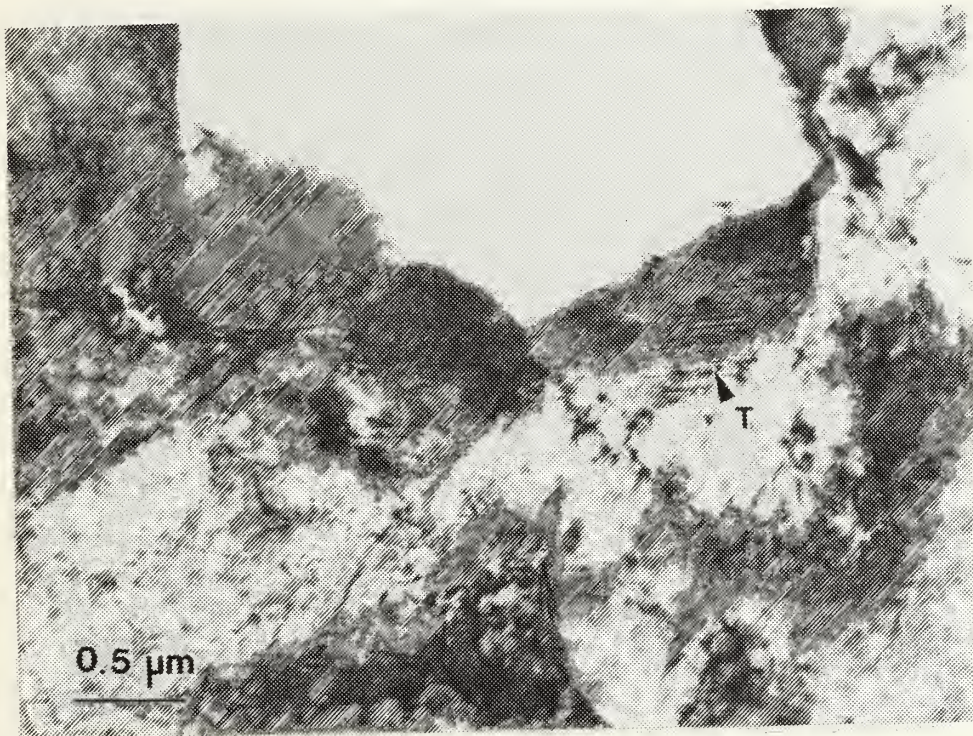


Figure 26. TEM Micrograph Showing Twins (T), 700 C Aged Material

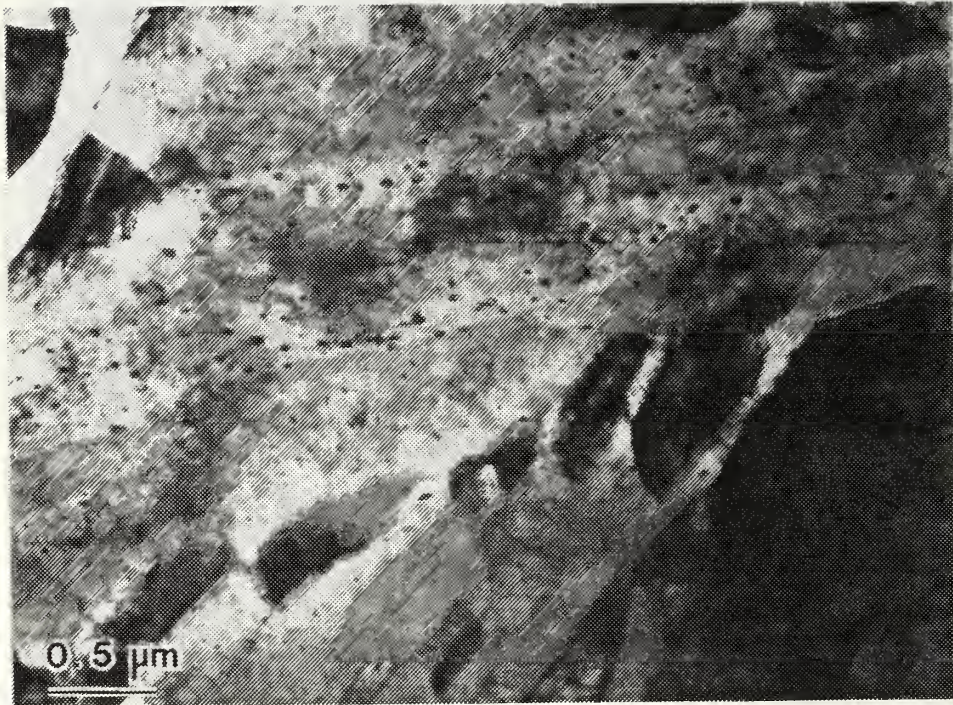


Figure 27. TEM Bright Field/Dark Field Micrographs Showing Coarse Copper Particles

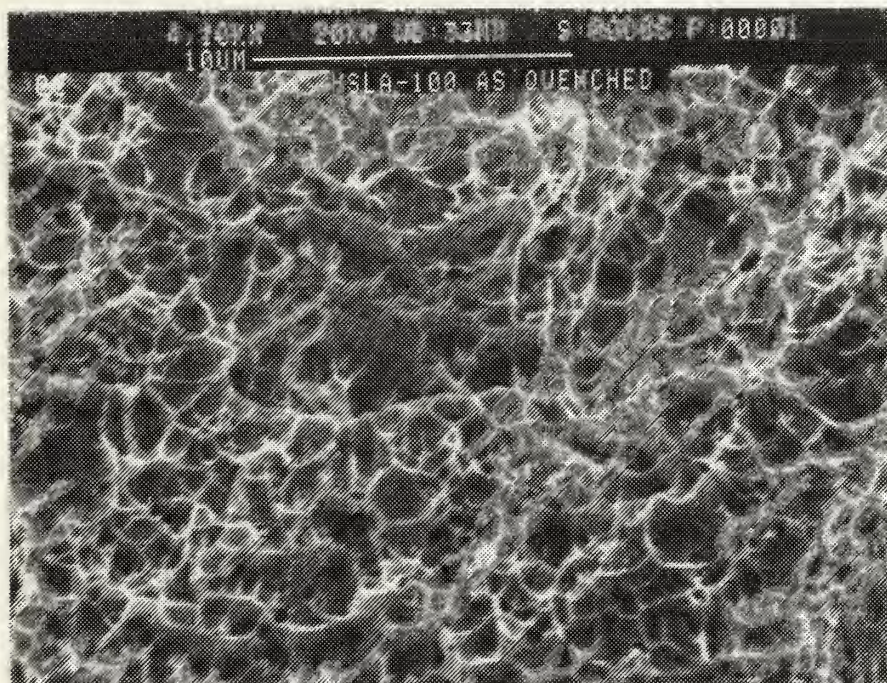
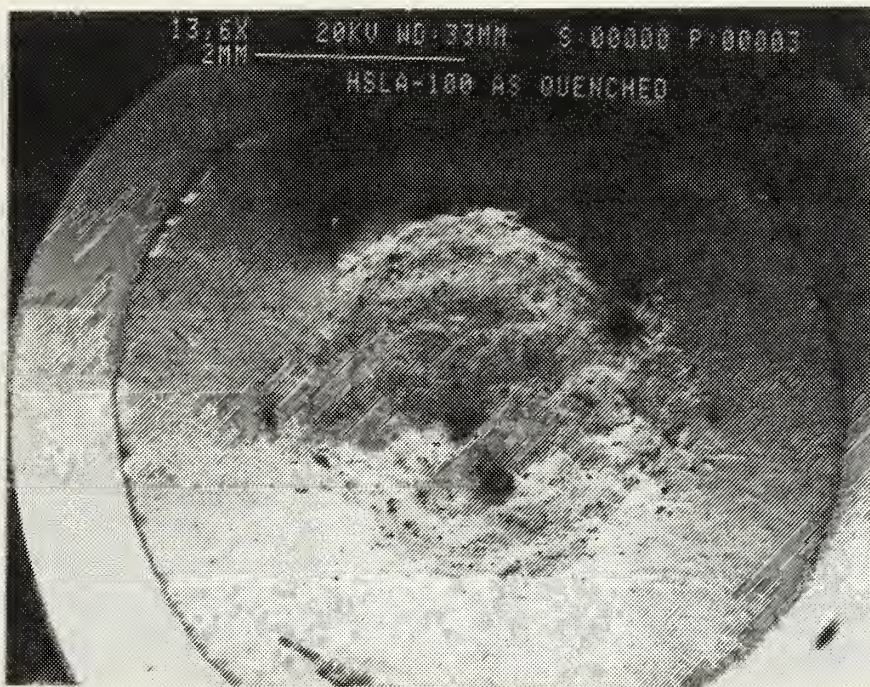


Figure 28. SEM Micrograph of As-Quenched Tensile Fracture Surface

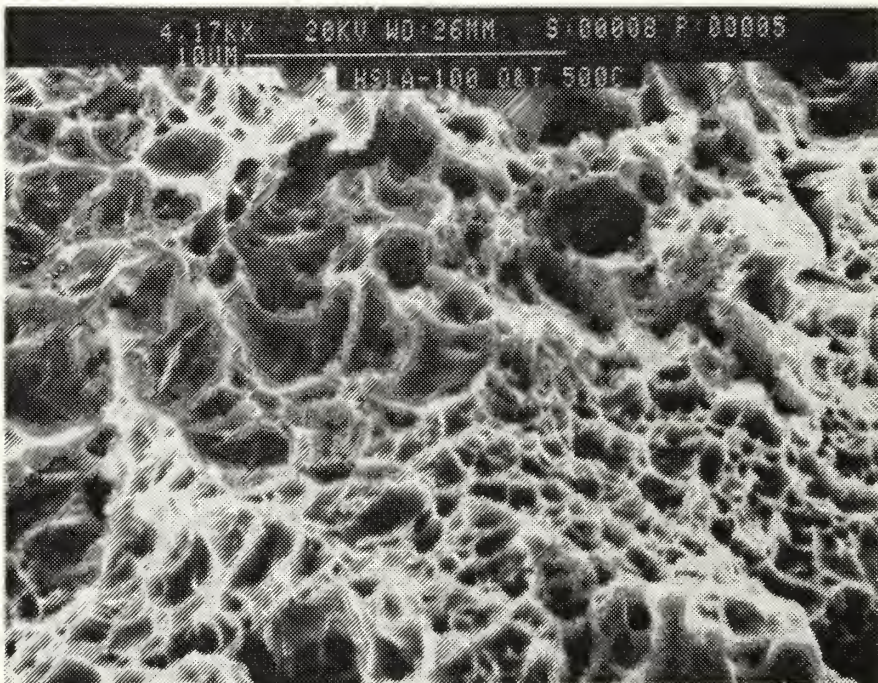
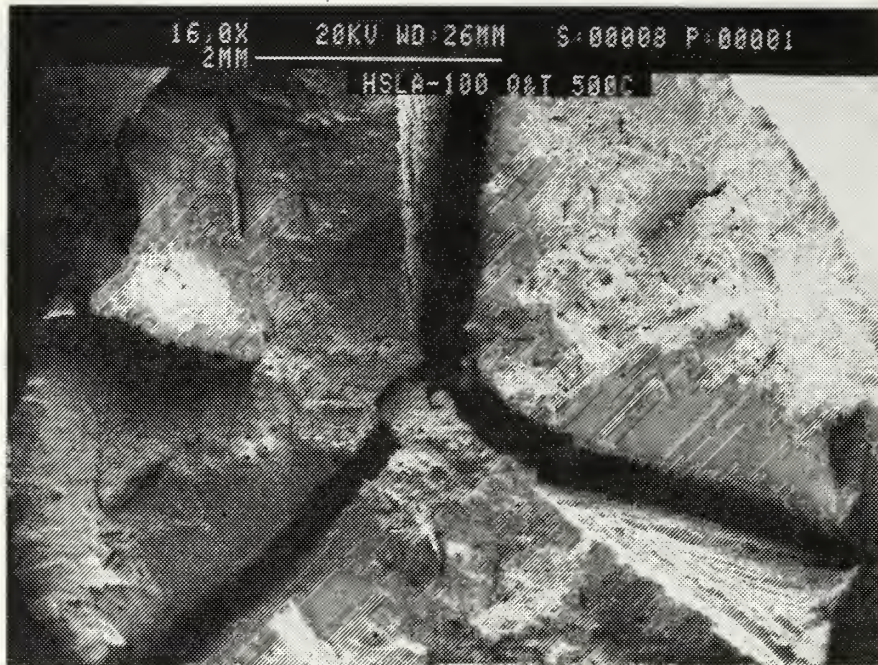


Figure 29. SEM Micrograph of 500 C Aging Temperature Tensile Fracture Surface

have been suggested. Elongated ferrite grains produced in rolling and grain-boundary segregation are causes of splitting which may be pertinent to this steel [Ref. 10]. The dimples are substantially larger in the 500 C aged sample than in the as-quenched material, indicating that the microvoid nucleation sites are more widely spaced as the microvoids have grown to a larger size before coalescing. The 650 C aged material (Figure 30) also exhibits splitting, although there is only one large split at this temperature. The dimples observed in the 650 C aged material were smaller than those observed after 500 C aging. The 700 C aged material (Figure 31) again exhibits the classic cup and cone fracture surface with deep dimples.

2. Charpy V-Notch Testing

The Charpy fracture surfaces in Figure 32 for the as-quenched material at 20 C and -85 C temperatures show inclusions which act as microvoid nucleation sites. Both temperatures show the dimples of a ductile fracture and are quite similar. The 500 C aged material (Figure 33) is the only condition which exhibits quasicleavage fracture characteristics in this Charpy testing. The room temperature (20 C) specimen shows both cleavage and small amounts of ductile tearing. The specimen fractured at -85 C is essentially a brittle fracture, although it has some very small areas where ductile tearing has taken place. The 650 C aged material (Figure 34) shows numerous inclusions and ductile tearing at both temperatures. The 700 C aged material (Figure 35) also indicates ductile tearing with large dimples

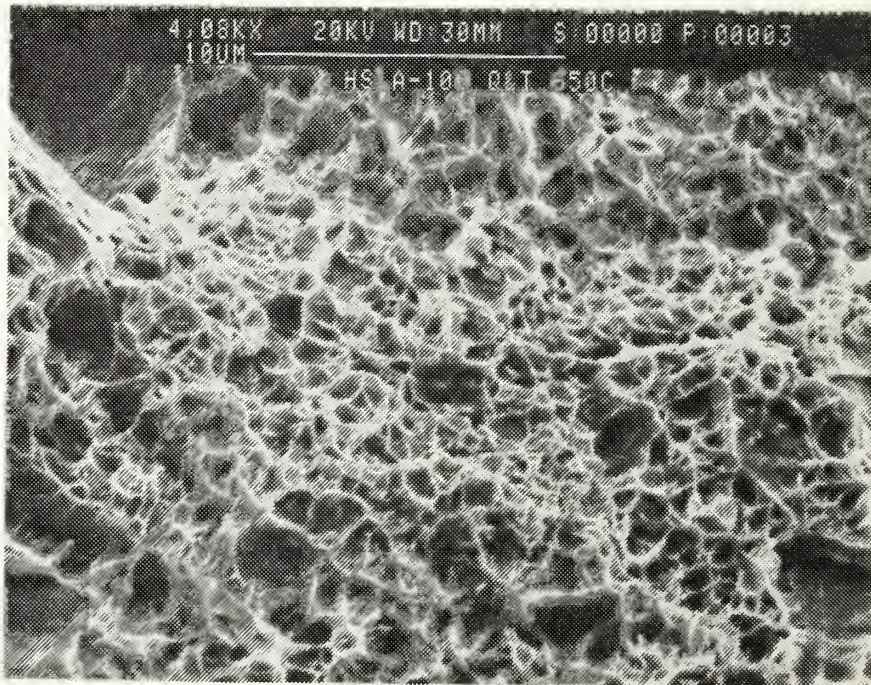
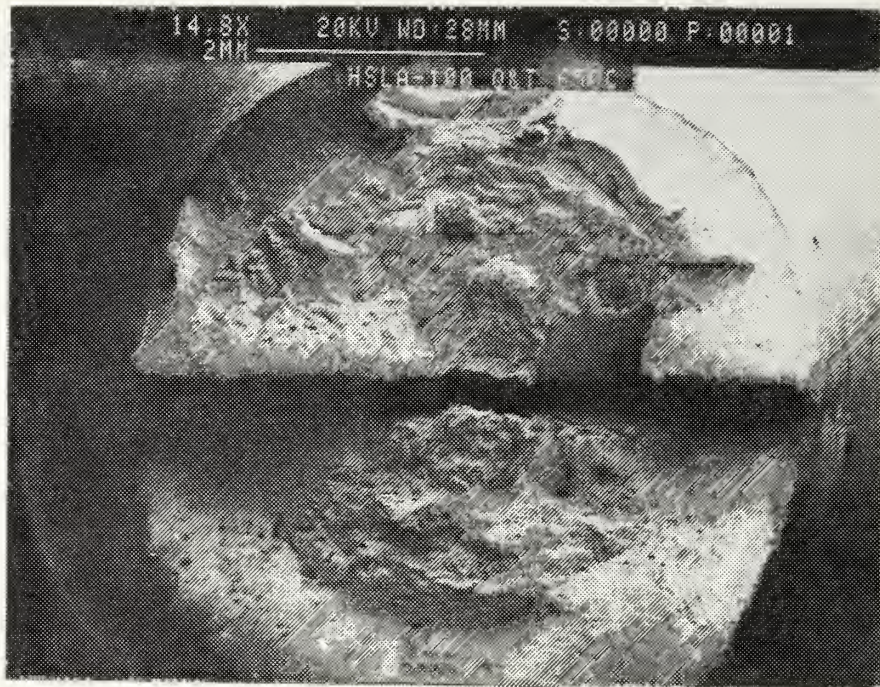


Figure 30. **SEM Micrograph of 650 C Aging Temperature
Tensile Fracture Surface**

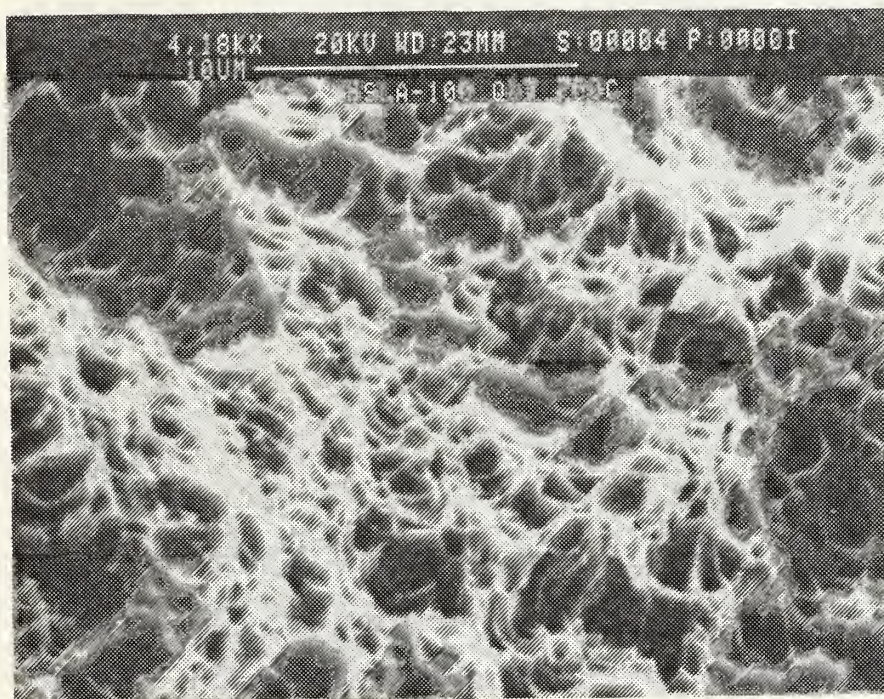
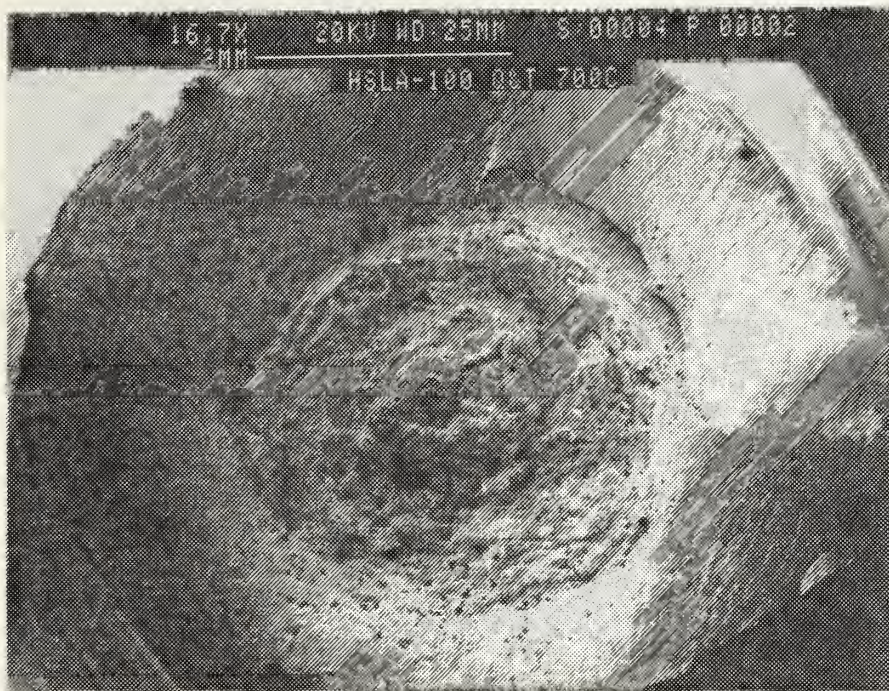


Figure 31. SEM Micrograph of 700 C Aging Temperature
Tensile Fracture Surface

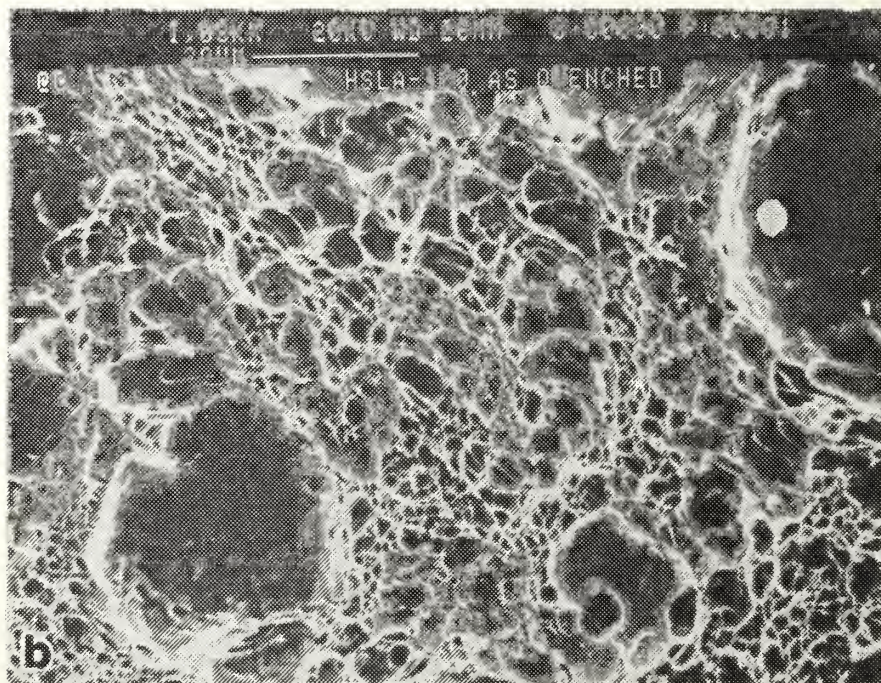
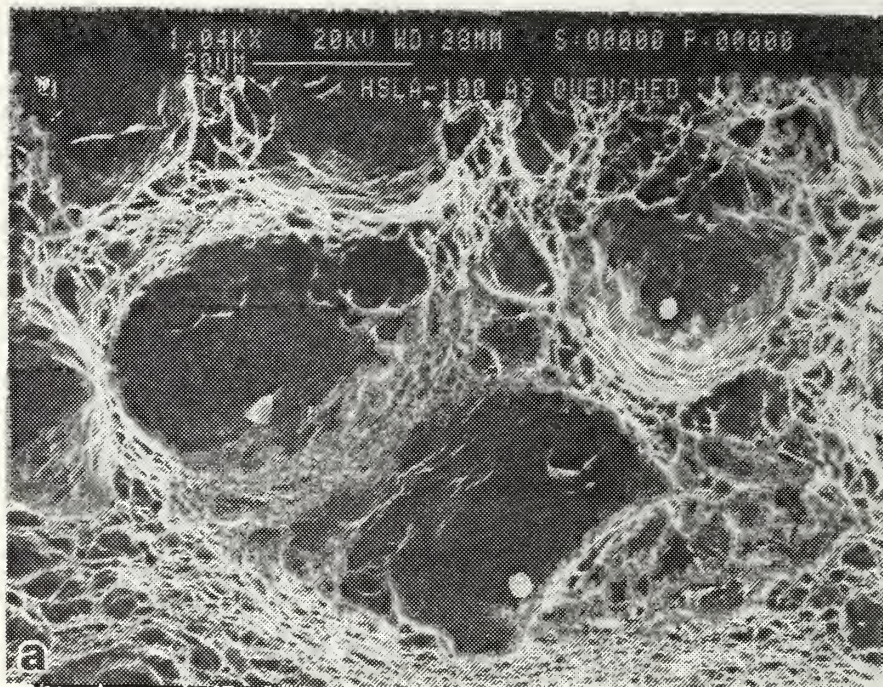
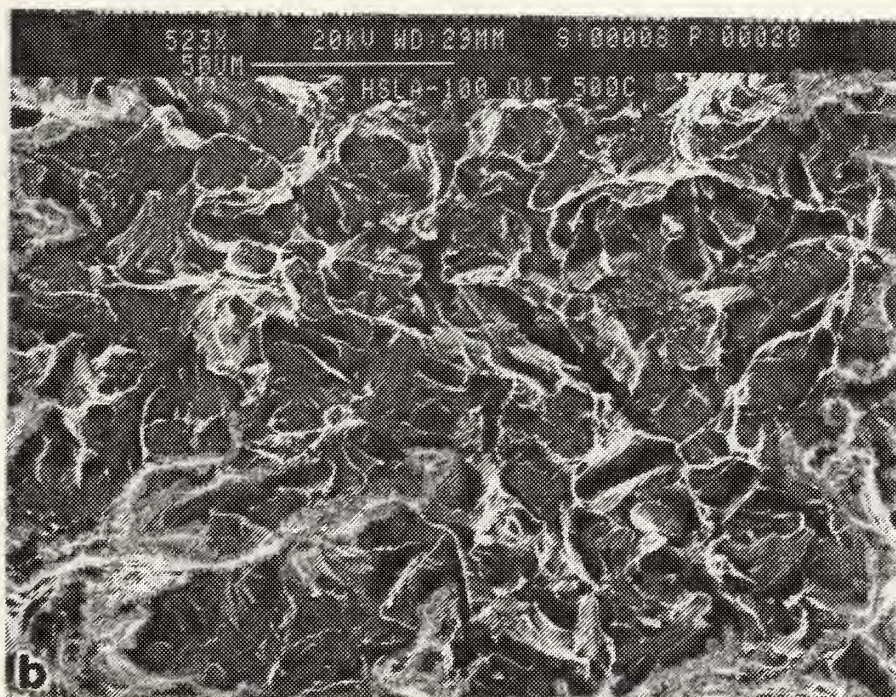
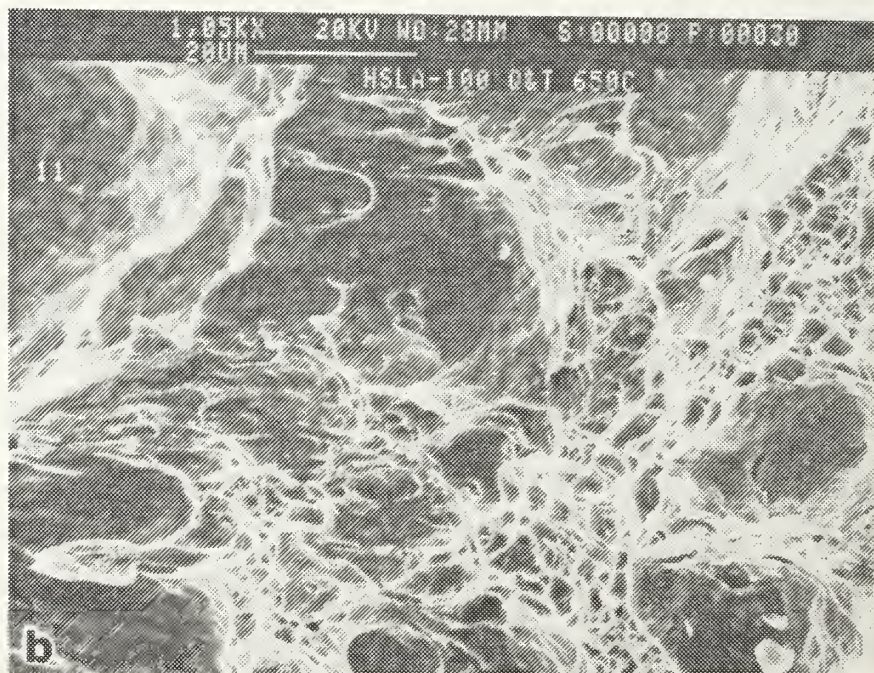
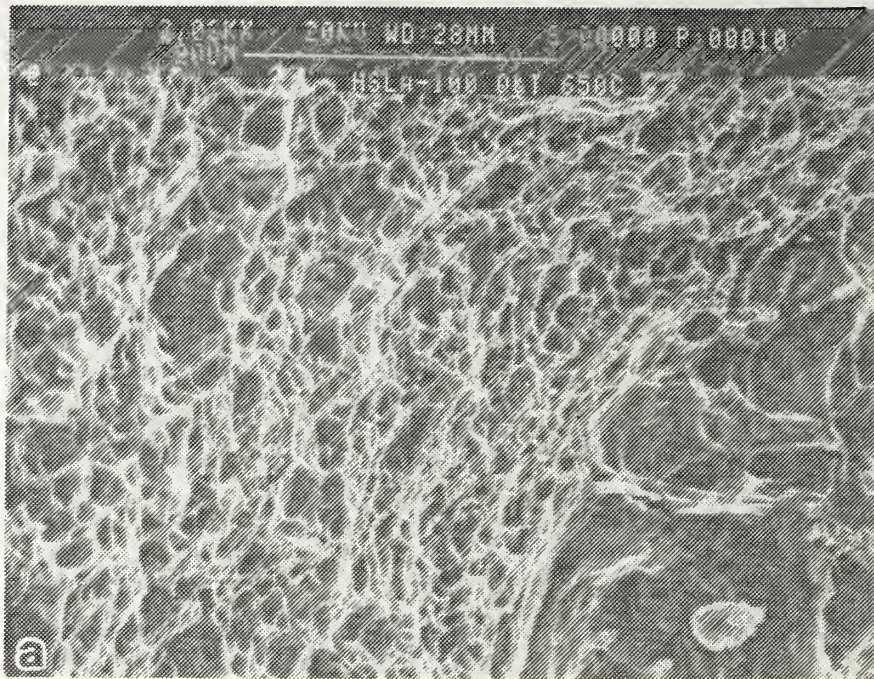


Figure 32. Charpy V-Notch Fracture Surface,
As-Quenched Material
(a) Fractured at -85 C; (b) Fractured at 20 C



**Figure 33. Charpy V-Notch Fracture Surface,
500 C Aged Material**
(a) Fractured at -85 C; (b) Fractured at 20 C



**Figure 34. Charpy V-Notch Fracture Surface,
650 C Aged Material**
(a) Fractured at -85 C; (b) Fractured at 20 C

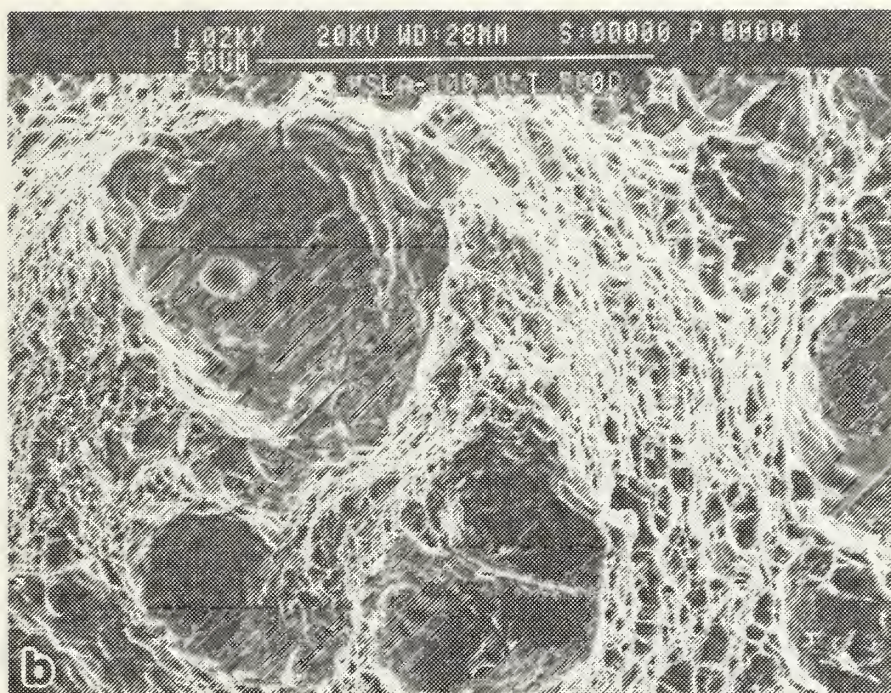
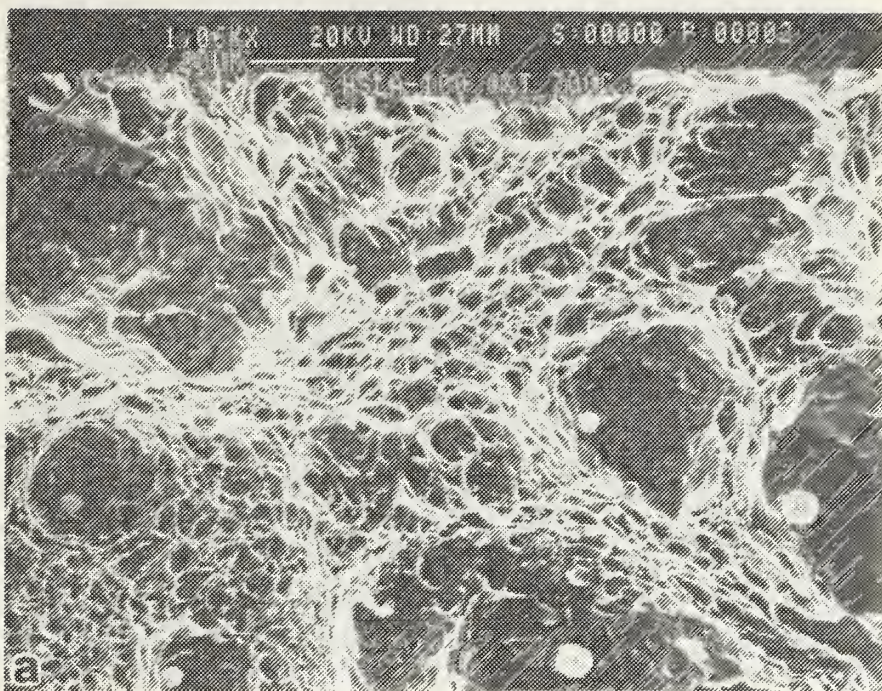


**Figure 35. Charpy V-Notch Fracture Surface,
700 C Aged Material
(a) Fractured at -85 C; (b) Fractured at 20 C**

at the inclusions. Splitting was not observed in any of the Charpy specimens. The absence of splitting can be attributed to the L-T orientation of these Charpy specimens.

A number of inclusion particles was selected for chemical analysis. The analysis of one particle is shown in Figure 36. This indicates that the inclusion particles are likely to be calcium sulfide. Calcium sulfide inclusions may be caused by the addition of calcium in the manufacturing process.

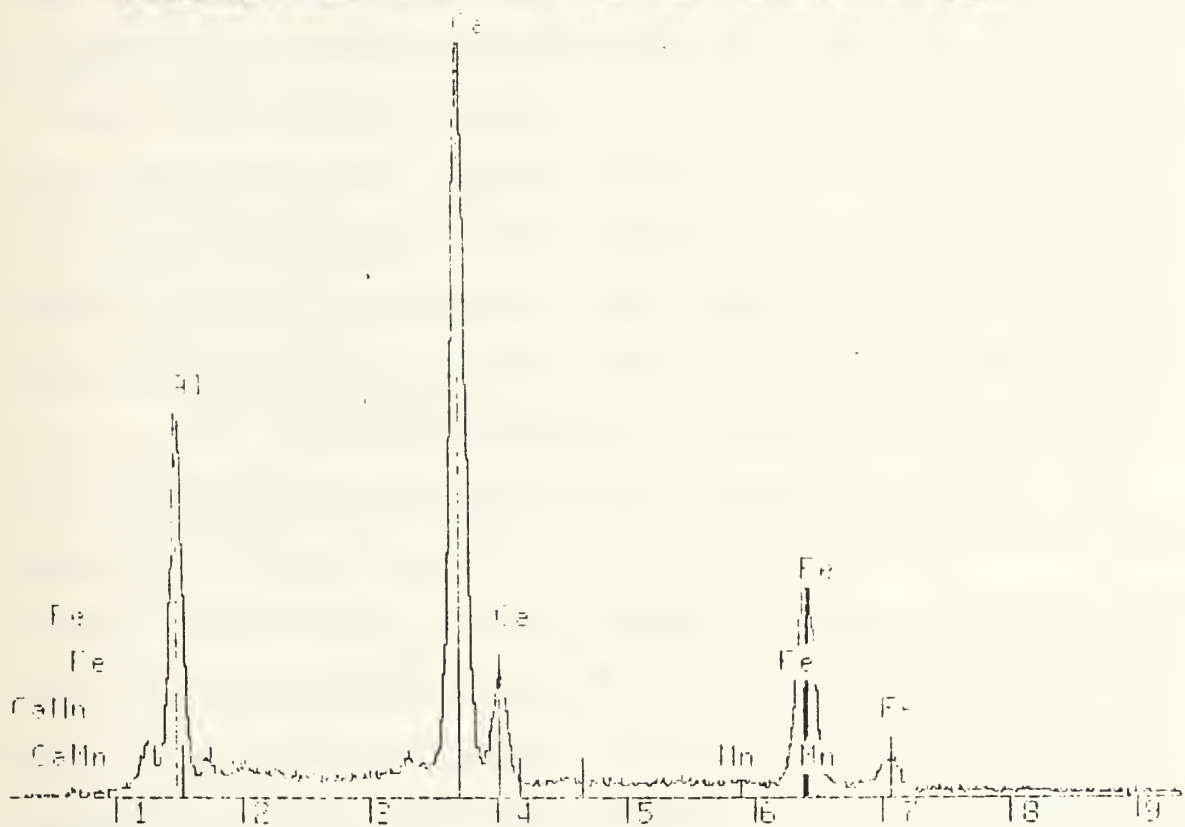
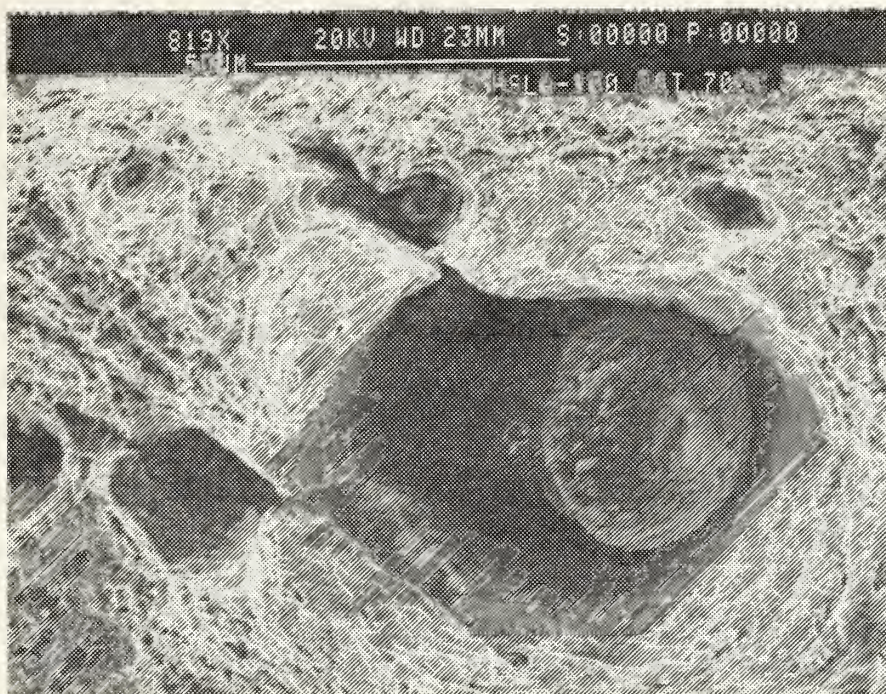


Figure 36. KEVEX Analysis of Chemical Composition of Inclusion, 700 C Aged Material

V. DISCUSSION

The good combination of strength and toughness observed in HSLA-100 steel can be attributed mainly to the fine grained bainitic microstructure produced in a quench and aging heat treatment. A significant source of the strengthening in as quenched bainitic steels is provided by a high dislocation density formed during the transformation from austenite to bainite. During aging of copper precipitation-strengthened HSLA steels, two main reactions take place. In the first, recovery of the dense dislocation substructure is lowering the strength. At the same time, precipitation of small copper particles tends to raise the strength through precipitation hardening. Another source of strengthening is the solid solution hardening provided by various alloying elements. Grain size refinement also plays an important role in strengthening this steel. Precipitation of niobium carbonitrides during the hot rolling process restrict the austenite grain size by retarding recrystallization and grain growth [Ref 19].

The increase in hardness and strength from the as-quenched to aged conditions can be related to the formation and growth of copper-rich clusters. The copper particles initially precipitate as coherent body centered cubic clusters [Ref. 8]. These clusters are very effective in restricting dislocation movement, increasing strength. As the copper particles grow by bulk diffusion, they transform into noncoherent, fine face centered cubic ϵ -phase copper [Ref. 19]. Continued growth of

the copper particles contributes to the decrease in the hardness and strength in overaged conditions. As the copper particles grow, the interparticle spacing is increased, which decreases the interaction of dislocations with the copper particles.

In this research, a maximum hardness and strength was reached at the 500 C aging temperature (Figures 4, 5). Although aging of the matrix reduced the number of dislocations as recovery took place (Figures 20, 24), dislocation density still provided a portion of the strengthening of HSLA-100 after this aging condition. The observations of Goodman [Ref. 9] indicate that fine (24 Å) copper provides significant strengthening at this temperature. The high hardness and strength values of this investigation support Goodman's work.

Two major factors contribute to the lower strength after the 650 C aging temperature (Figures 5, 6). After 650 C aging, the copper precipitates were coarser (100–600 Å), providing less strengthening effect than did the fine (24 Å) copper precipitates [Ref. 9]. Dislocations provided less strengthening than after 500 C aging because dislocation recovery was more advanced. A rod-like growth in the coarser copper particles, as was found by Hornbogen [Ref. 6] and Speich [Ref.7], can be seen at this temperature (Figure 22).

After the 700 C aging, the yield strength was further decreased. The copper precipitates have grown to a very coarse size (up to 1,000 Å). These coarse copper particles were elongated and found in higher densities along the lath and grain boundaries. The dislocation density was low after 700 C aging, having only a minor role in strengthening.

After this aging, a significant amount of martensite/austenite was preferentially formed on the grain and lath boundaries. Although the copper-iron phase diagram shows the eutectoid temperature at 850 C (Figure 2), the changes in the trends of the mechanical properties and the greatly increased amounts of martensite/austenite indicate that the eutectoid temperature has been significantly lowered by the presence of other alloying elements. Andrews' formula [Ref. 20] was used to calculate a eutectoid temperature of 671 C. However, Andrews' formula does not take into account the effect of copper on the eutectoid temperature. This calculated value is quite close to the 680 C which Coldren [Ref. 18] experimentally determined for a similar steel. The observations of this investigation are in good agreement with these values.

The occurrence of the eutectoid temperature near 680 C may explain the alteration in the mechanical properties which occurred at this point. Figure 7 shows that HSLA-100 is most ductile after the 675 C aging temperature, but the ductility decreases after 700 C aging. This may be attributed to the formation of a significant number of martensite/austenite particles formed during the 700 C aging. The martensite/austenite microconstituent can be more brittle than the ferrite matrix, which caused a reduction in ductility.

As indicated in previous work [Refs. 3, 8, 9], the most desirable strength and ductility properties for low carbon copper precipitation strengthened steels are reached in an overaged condition. Figure 37

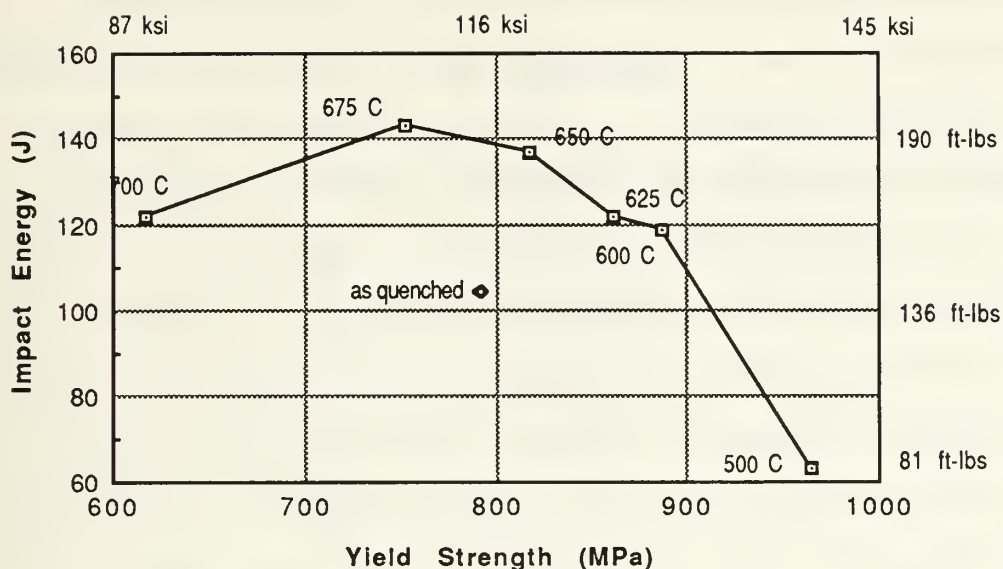


Figure 37. **The Relationship of Notch Toughness and Yield Strength**

illustrates the relationship of the impact energy and the yield strength for various aging temperatures. The 675 C aging temperature provided the greatest ductility while meeting the Navy strength requirements (see Appendix). If, however, the HSLA-100 eutectoid temperature is in fact near 680 C, the use of 675 C as an optimum aging temperature for processing would not be advisable. Variations in temperature could easily allow the steel to move into the two-phase region above the eutectoid temperature and mechanical properties would become much less predictable.

Splitting in the rolling direction has been investigated and possible explanations were suggested in previous research [Refs. 21, 22]. In the fractographs of the tensile specimens, it can be seen that splitting

occurs at the aging temperatures from 500 C to 675 C (Figures 29, 30). Although previous work [Refs. 21, 22] has associated the splitting with cementite precipitates on the ferrite boundaries, cementite is not present in significant amounts in this steel. The actual causes of splitting are the subject of some controversy. Apparently, the elongation of grains in the rolling direction, segregation of impurities along the grain boundaries, and the development of an unfavorable crystallographic texture all have an influence on splitting. The presence of splitting did not seem to have an adverse effect on this material's mechanical properties but is an area that needs further investigation.

VI. SUMMARY

The effect of aging temperature on the microstructure and mechanical properties of 25.4 mm thick HSLA-100 steel was studied. A fine grain structure, dislocation density, and niobium carbonitride precipitation were found to provide the strengthening in the as-quenched condition. As this material is aged, fine copper particles precipitate and provide significant strengthening. After 500 C aging, a maximum yield strength of 965 MPa and a room temperature Charpy impact energy of 108 J were observed. Very fine, uniformly distributed coherent copper precipitates are causing maximum strength for this treatment. Aging temperatures up to 675 C resulted in a decrease in yield strength with an increase in impact energy. Aging at 675 C gave the highest impact energy (143 J at 20 C) and a yield strength over 690 MPa (100 ksi). Significant coarsening in the copper precipitates was observed over this range of treatments. An aging temperature of 700 C produced lower yield strengths and impact energies than at 675 C aging. This was associated with the formation of brittle martensite/austenite particles along the ferrite boundaries, suggesting that this temperature is in a two phase region.

Splitting of the tensile specimens was observed in the intermediate aging temperatures and is not quite understood.

APPENDIX

SPECIFICATION CHEMICAL COMPOSITION AND MECHANICAL PROPERTY REQUIREMENTS FOR NAVAL HULL MATERIALS

	BASE METALS				
	HY-80 MIL-S-16216J (10 Apr 81)	HY-100 MIL-S-16216J (10 Apr 81)	HY-130 MIL-S-24371A (21 Aug 75)	HSLA-80 MIL-S-24645 (4 Sep 1984)	HSLA-100 Interim Specification (Apr 1986)
C	.10/.20	.10/.22	.12	.07	.06
Mn	.10/.45	.10/.45	.60/.90	.40/.70	.75/1.05
Si	.12/.38	.12/.38	.15/.35	.40	.40
P	.020	.020	.010	.025	.015
S	.002/.020	.002/.020	.010	.010	.006
Ni	1.93*/3.32	2.18*/3.57	4.75/5.25	.70/1.00	3.35/3.65
Mo	.17*/.63	.17*/.63	.30/.65	.15/.25	.55/.65
Cr	.94*/1.86	.94*/1.86	.40/.70	.60/.90	.45/.75
V	.03	.03	.05/.10	—	—
Al	—	—	—	.015	.02/.04
Ti	.02	.02	.02	—	—
Cu	.25	.25	.25	1.00/1.30	1.45/1.75
Others	Ar, Sn, Sb	Ar, Sn, Sb	—	Ar, Sb	N, Cb
Fe	Balance	Balance	Balance	Balance	Balance
Yield Strength 0.2% Offset, ksi	80/99.5*	100/115*	130/150*	80/99.5	100/115*
Tensile Strength, ksi	—	—	—	—	—
Elongation in 2-inches, %	20*	18*	15*	20*	18*
CVN Impact, Energy, ft-lb	35@ -120° F 60@ 0° F	30@ -120° F 55@ 0° F	60@ 0° F 60@ R.T.	35@ -120°F 60@ 0°F	30@ -120°F 55@ 0°F
DT Impact Energy, ft-lb	450@ -40° F	500@ -40° F	500@ 0° F	450@ -40°F	—

*Requirement varies with thickness

LIST OF REFERENCES

1. Anderson, T. L., Hyatt, J. A., and West, J. C., "The Benefits of New High-Strength Low-Alloy (HSLA) Steels," *Welding Journal*, pp. 21-26, September 1987.
2. David Taylor Research Center, Report TM-28-88/03, *Certification of HSLA-100 Steel for Structural Applications*, by E. Czyryca, R. Link, and R. Wong, pp. 1-104, January 1988.
3. Hamburg, E. G., and Wilson, A. D., "Production and Properties of Copper, Age Hardened Steels," paper presented at the TMS AIME International Symposium, Pittsburg, PA, November 3-5, 1987.
4. AMAX Materials Research Center, Report CPR-20, *Development of 100 KSI Yield Strength HSLA Steel*, by A. P. Colden and T. B. Cox, pp. 2-6, July 1986.
5. LeMay, I., Schetky, L., and Krishnadev, M. R., "The Role of Copper in HSLA Steels: A Review and Update," *High Strength Low Alloy Steels*, pp. 64-67, August 1984.
6. Hornbogen, E., and Glenn, R. C., "A Metallurgical Study of Precipitation of Copper from Alpha Iron," *Transactions of the Metallurgical Society of AIME*, v. 218, pp. 1064-1070, December 1960.
7. Speich, G. R., and Oriani, R. A., "The Rate of Coarsening of Copper Precipitate in Alpha-Iron Matrix," *Transactions of the Metallurgical Society of AIME*, v. 233, pp. 623-631, April 1965.
8. Goodman, S. R., Brenner, S. S., and Low, J. R., "An FIM-Atom Probe Study of the Precipitation of Copper from Iron-1.4 At. Pct. Copper. Part I: Field Ion Microscopy," *Metallurgical Transactions*, v. 4, pp. 2363-2370, October 1973.
9. Goodman, S. R., Brenner, S. S., and Low, J. R., "An FIM-Atom Probe Study of the Precipitation of Copper from Iron-1.4 At. Pct. Copper. Part II: Atom Probe Analyses," *Metallurgical Transactions*, v. 4, pp. 2371-2378, October 1973.
10. *Metals Handbook*, 9th ed., v. 12, pp. 104-106, American Society for Metals, 1987.

11. Kvidahl, L. G., "An Improved High Yield Strength Steel for Shipbuilding," *Welding Journal*, v. 64, pp. 42-48, July 1985.
12. Wilson, A. D., "High Strength Weldable Precipitation Aged Steels," *Journal of Metals*, v. 39, pp. 36-38, March 1987.
13. Pickering, F. B., *Physical Metallurgy and the Design of Steels*, pp. 60-87, Applied Science Publishers Ltd., 1978.
14. LeMay, I., and Krishnadev, M. R., *Copper in Iron and Steel*, pp. 5-43, 83-133, Wiley-Interscience, 1982.
15. David Taylor Research Center, Report SME-87/83, *Trial Production of HSLA-100 Steel Plate*, by Ernest J. Czyryca, pp. 2-22, February 1988.
16. Thompson, S. W., Colvin, D. J., and Krauss, G., "On the Bainitic Structure Formed in a Modified A710 Steel," *Scripta Metallurgica*, v. 22, pp. 1069-1074, July 1988.
17. Bush, M. E., and Kelly, P. M., "Strengthening Mechanisms in Bainitic Steels," *Acta Metallurgica*, v. 19, pp. 1363-1371, December 1971.
18. Wilson, A. D., Hamburg, E. G., Thompson, S. W., Colvin, D. J., and Krauss, G., "Properties and Microstructures of Copper Precipitation Aged Plate Steels," paper presented at Microalloying '88, Chicago, Illinois, September 24-29 1988.
19. Miglin, M. T., Hirth, J. P., Rosenfield, A. R., and Clark, W. A., "Microstructure of a Quenched and Tempered Cu-Bearing High Strength Low-Alloy Steel," *Metallurgical Transactions*, v. 17A, pp. 791-798, May 1986.
20. Andrews, K. W., "Empirical Formulae for the Calculation of Some Transformation Temperatures," *Journal of the Iron and Steel Institute*, pp. 721-727, July 1965.
21. Hero, H., Evensen, J., and Embury, J. D., "The Occurrence of Delamination in a Control Rolled Steel," *Canadian Metallurgical Quarterly*, v. 14, pp. 117-122, 1975.
22. DeArdo, A. J., "An Investigation of the Mechanism of Splitting Which Occurs in Tensile Specimens of High Strength Low Alloy Steels," *Metallurgical Transactions*, v. 8A, pp. 473-486, March 1977.

INITIAL DISTRIBUTION LIST

	<u>No. Copies</u>
1. Defense Technical Information Center Cameron Station Alexandria, VA 22304-6145	2
2. Library, Code 0142 Naval Postgraduate School Monterey, CA 93943-5002	2
3. Department Chairman, Code 69Hy Department of Mechanical Engineering Naval Postgraduate School Monterey, CA 93943-5000	1
4. Dr. Saeed Saboury P. O. Box 51922 Pacific Grove, CA 93950	2
5. Dr. J. M. B. Losz, Code 69Lo Department of Mechanical Engineering Naval Postgraduate School Monterey, CA 93943-5000	3
6. Professor T. R. McNelley, Code 69Mc Department of Mechanical Engineering Naval Postgraduate School Monterey, CA 93943-5000	1
7. Mr. Paul W. Holsberg, Code 2815 David Taylor Naval Ship Research and Development Center Annapolis, MD 21402-5067	1
8. Mr. E. J. Czyryca, Code 2814 David Taylor Naval Ship Research and Development Center Annapolis, MD 21402-5067	1

- | | | |
|-----|--|---|
| 9. | Capt. S. McNutt, CF
13 Paula Crescent
Nepean, Ontario, Canada K2H 8Y8 | 1 |
| 10. | Lt. M. H. Heinze, USN, Code N64
Commander Naval Surface Force, U.S. Pacific Fleet
NAB Coronado
San Diego, CA 92155-5035 | 2 |

Thesis
H4237
c.1

Heinze
The effect of aging
treatment on the micro-
structure and properties
of copper-precipitation
strengthened HSLA steel. 1.

Thesis

H4237 Heinze

c.1 The effect of aging
treatment on the micro-
structure and properties
of copper-precipitation
strengthened HSLA steel.



thesH4237

The effect of aging treatment on the mic



3 2768 000 81327 3

DUDLEY KNOX LIBRARY